**Przemysław Kolek, PhD**
**PhD on chemistry**

Rzeszów, 21.12.2020

# SELF-PRESENTATION

# *From the laser-induced fluorescence spectra to geometry and dynamics of excited molecules: investigations of anthranilic acid molecules cooled in supersonic molecular beam*

Presentation of scientific achievements and results
in connection with applying for
the of the habilitation degree
in the discipline of Chemical Sciences

Rzeszów
2020

## TABLE OF CONTENT:

# I. PERSONAL DATA, DEGREES, DIPLOMAS AND THE COURSE OF SCIENTIFIC CAREER TO DATE

## 1.1. PERSONAL DATA, ACADEMIC DEGREES AND DIPLOMAS

### *DANE PERSONALNE:*

| | |
|---|---|
| **Full name:** | **Przemysław Kolek (Przemysław Jan Kolek)** |
| **ORCID number:** | **0000-0003-3838-5172** |
| **Degree:** | **PhD in Chemical Sciences** |
| **Official address:** | **University of Rzeszów**<br>College of Natural Sciences<br>Institute of Physics<br>1 Prof. Pigonia Street<br>35-310 Rzeszów, Poland |
| Office phone: | +48 17 851-86-99 |
| e-mail: | pkolek@ur.edu.pl |

### *DEGREES AND DIPLOMAS:*

**PhD in Chemical Sciences:** Jagiellonian University, Cracow, 2003.
**PhD with honours**

| | |
|---|---|
| Title of doctoral dissertation: | *“Widma elektronowo-oscylacyjne schłodzonych cząsteczek cyjanowych pochodnych aniliny”* |
| Translation of the tilte: | *“Vibronic spectra of cooled molecules of cyano-derivatives of aniline"* |
| Promoter: | prof. dr hab. Jan Najbar |

**Master of Science in Chemistry:** Jagiellonian University, Cracow 1997 r.

| | |
|---|---|
| Title of master thesis: | *“Badania stanów wzbudzonych wybranych wielopodstawionych pochodnych benzenu”* |
| Translation of the tilte: | *“Studies on excited states of selected multi-substituted benzene derivatives”* |
| Promoter: | prof. dr hab. Jan Najbar |

## I.2. THE COURSE OF SCIENTIFIC CAREER AND SCIENTIFIC ACTIVITY IN VARIOUS SCIENTIFIC CENTRES, INCLUDING FOREIGN ONES

### *THE COURSE OF SCIENTIFIC CAREER TO DATE*

Information on employment to date in scientific or artistic institutions

| | |
|---|---|
| 01.10.1997 –<br>30.09.1998 | Assistant traineeship at the Jagiellonian University (Cracow, Poland), at the Faculty of Chemistry at the Department of Physical Chemistry and Electrochemistry, in the Group of Photochemical and Luminescence Studies |

| | |
|---|---|
| 01.10.1998 – 28.02.2003 | PhD studies at the Jagiellonian University (Cracow, Poland),<br>at the Faculty of Chemistry at the Department of Physical Chemistry and Electrochemistry, in the Group of Photochemical and Luminescence Studies. |
| 17.03.2003 – 31.07.2005 | Postdoctoral contract at the University of Basel (Switzerland),<br>in the Institute of Physical Chemistry, in the Astrochemistry Group,<br>Head: Prof. Dr. John P. Maier |
| 01.10.2005 – 30.09.2009 | Employment as an assistant at the Jagiellonian University (Cracow, Poland),<br>at the Faculty of Chemistry at the Department of Physical Chemistry and Electrochemistry, in the Group of Photochemical and Luminescence Studies. |
| Since 01.10.2006 to date | Employment as an adjunct professor at the University of Rzeszów (Rzeszow, Poland), at the Institute of Physics at the Faculty of Mathematics and Natural Sciences, and since 01.10.2019 at the College of Natural Sciences, Institute of Physics, since 01.10.2018 as a senior lecturer/ lecturer in a teaching group |

### *INTERNSHIPS AND SCIENTIFIC CONTRACTS, FOREIGN AND DOMESTIC*

Information on significant scientific activity carried out in more than one scientific institution, in particular abroad

| | |
|---|---|
| 17.03.2003 – 31.07.2005 | Postdoctoral contract at the University of Basel (Switzerland),<br>in the Institute of Physical Chemistry,<br>in the Astrochemistry Group,<br>Head: Prof. Dr. John P. Maier |
| 01.12.2003 – 29.02.2004 | Postdoctoral internship at the Université Paris-Est Marne la Vallée (Paris, France) in the Laboratory of Theoretical Chemistry<br>postdoctoral internship within the European program:<br>*Marie Curie Research Training Network, Theonet II,*<br>Head: Prof. Dr. Pavel Rosmus |
| 15.09.2008 – 30.09.2008 | Internship at the Institute of Physics of the Polish Academy of Sciences (Warsaw),<br>in the Department of Radiation Physics and Spectroscopy,<br>in the Group of Molecular Photophysics;<br>Head of the internship: prof. dr hab. Andrzej L. Sobolewski |
| 01.10.2009 – 31.01.2010 | Scientific internship at the Jagiellonian University<br>at the Faculty of Chemistry in the Department of Physical Chemistry and Electrochemistry, in the Femtochemistry Group,<br>Head of the internship:: dr hab. Marek Mac |

# II. OVERVIEW OF THE SCIENTIFIC ACHIEVEMENT

**Description of the achievements set out in art. 219 para 1 point 2 of the Act.**

## II.1 PUBLICATIONS CONSTITUTING THE SCIENTIFIC ACHIEVEMENT

Below the IF for the year of publication and the current citation number according to the Scopus database are listed as well as the scoring pinots of the Polish Ministry of Science and Higher Education MNiSW

H1. Katarzyna Pirowska, Przemysław Kolek, Jakub Goclon, Jan Najbar*
*"Geometry changes upon $S_0$–>$S_1$ electronic excitation of aniline derivatives"*
*CHEMICAL PHYSICS LETTERS*, Vol. 387 (2004) 165-175
IF = 2,438, Cyt = 13, MNiSW scoring(old[b])= 25, MNiSW scoring(new[c]) = 70

H2. Przemysław Kolek*, Sebastian Leśniewski, Katarzyna Pirowska, Jan Najbar
*„LIF excitation spectra for S0 –> S1 transition of anthranilic acid: Detailed studies"*
*JOURNAL OF MOLECULAR SPECTROSCOPY, Vol. 249 (2008) 100–112*
IF = 1,636, Cyt = 6 MNiSW scoring(old)= 25, MNiSW scoring(new)= 70

H3. Sebastian Leśniewski, Przemysław Kolek*, Katarzyna Pirowska, Andrzej L. Sobolewski, Jan Najbar
*„Franck–Condon analysis of laser-induced fluorescence excitation spectrum of anthranilic acid: Evaluation of geometry change upon $S_0$ –> $S_1$ excitation"*
*JOURNAL OF CHEMICAL PHYSICS*, Vol. 130, (2009) 054307-1–054307-14,
IF = 3,093, Cyt = 16 MNiSW scoring(old)= 35, MNiSW scoring(new) = 100

H4. Przemysław Kolek*, Sebastian Leśniewski, Marcin Andrzejak, Maciej Góra, Paweł Cias, Adam Węgrzynowicz, Jan Najbar,
*„LIF excitation spectra for $S_0 \rightarrow S_1$ transition of deuterated anthranilic acid COOD, $ND_2$ in supersonic-jet expansion",*
*JOURNAL OF MOLECULAR SPECTROSCOPY*, Vol. 264 (2010) 129–136,
IF = 1,497, Cyt = 5 MNiSW scoring(old)= 25, MNiSW scoring(new)= 70

H5. Przemysław Kolek*, Marcin Andrzejak, Jan Najbar, Małgorzata Ostrowska-Kopeć, Izabela Piotrowska,
*"Isotopic effects in the $S_1$ exited state of anthranilic acid deuterated in various positions in substituent groups. Supersonic-jet LIF spectroscopy and CC2 ab initio study"*
*CHEMICAL PHYSICS*, Vol. 450 (2015) 46-58,
IF = 1,758, Cyt = 2 MNiSW scoring(old)= 25, MNiSW scoring(new) = 70

H6. Przemysław Kolek*, Marcin Andrzejak, Rafał Hakalla, Wojciech Szajna,
*"Quantitatively adequate calculations of the H-chelate ring distortion upon the in the $S_0$-$S_1(\pi\pi^*)$ excitation in internally H-bonded o-anthranilic acid: CC2 coupled cluster versus TDDFT"*
*JOURNAL OF PHYSICAL CHEMISTRY A*, Vol. 122 (2018) 6243-6255
IF = 2,836, Cyt = 3 MNiSW scoring(old)= 30, MNiSW scoring(new)= 100

H7. Przemysław Kolek*, Marcin Andrzejak, Tomasz Uchacz, Paweł Szlachcic
*"Consistent Franck-Condon modeling of geometry changes for the $S_0 \rightarrow S_1(\pi\pi^*)$ excitation in anthranilic acid: LIF spectroscopy aided by CC2 or TDDFT vibrations."*
*JOURNAL OF QUANTITATIVE SPECTROSCOPY & RADIATIVE TRANSFER,*
Vol. 242 (2020), 106747 (pgs. 1-16)
IF = 2,955, Cyt = 1 MNiSW scoring(old) = 35, MNiSW scoring(new) = 100

* asterisk indicates the corresponding author for the publication concerned

[b] – MNiSW scoring(old[b]) – is the number of scoring points of the Polish Ministry of Science and Higher Education (MNiSW) according to values valid until 2018.

[c] – MNiSW scoring(new[b]) – is the number of scoring points of the Polish Ministry of Science and Higher Education (MNiSW) according to values valid since 2019.

## II.2. INTRODUCTION

### *II.2.1. RESEARCH OBJECTIVE AND MOTIVATION*

**The aim of this study is to investigate the geometry and dynamics of the anthranilic (*ortho*-aminobenzoic) acid molecule in the first singlet excited state S1(π→π*), and to quantify the changes in equilibrium geometry caused by excitation to this state, based on experimental results. In particular, determination of the changes associated with significant strengthening of the N–H···O intramolecular hydrogen bond and deformation of the substitutes that form them due to the excitation.**

The investigated changes are associated with intramolecular hydrogen atom dislocation, related to the phenomenon of excited-state intramolecular proton transfer ESIPT, often causing the emission of strongly stokes-shifted dual fluorescence. These phenomena are thoroughly studied both because of their importance for photochemistry and spectroscopy, as well as their importance in biological and medical sciences as well as potential applications in molecular engineering, nanotechnology and optoelectronics, for the production of molecular switches. One of the groups of molecules in which these phenomena occur are α-hydroxyl derivatives of carbonyl compounds, in which functional groups are connected with the conjugated π-electronic system. The best-known research concerns the dual fluorescence of salicylic acid molecules and its derivatives, but since the late of the 20th century, anthranilic acid and its derivatives have also been investigated in this respect, largely due to its importance as a fluorescent molecular probe for protein systems.

Studies on geometry and dynamics of molecules in excited electron states are important issues of molecular spectroscopy and photochemistry because they provide insight into the properties of excited molecules and into the changes induced by electronic excitation. The frequencies of oscillations in the excited state provide valuable information about the dynamics of the molecule, especially about the force constants of bonds, and consequently, the so-called bond strength. In turn, the changes of these quantities are very sensitive, differential indicators of changes of the molecular dynamics upon the excitation. Similarly, due to the correlation between the bond lengths and the so-called bond strength, their multiplicity, energy and force constants, studies of changes in molecular geometry indirectly provide information about these quantities, as well as localization/delocalization of bonds, and thus also the electronic structure, the properties and chemical reactivity of molecules in excited states. Experimental investigations of the above issues are only possible with the use of advanced molecular spectroscopy methods, because of the short lifetime of molecules in excited states and the very small occupation numbers of these states make it impossible to use the methods commonly used for base state molecules.

### *II.2.2. IMPORTANCE AND PECULIARITY OF EXCITED-STATE GEOMETRY STUDIES*

Accurate determination of the geometry of molecules in excited states is possible by means of high-resolution UV-vis spectroscopy with rotational resolution. Unfortunately, in practice this is only possible for molecules consisting of several atoms. Differences in the equilibrium geometry between the ground and excited states for molecules consisting of dozen or so atoms can be determined on the basis of the analysis of the intensities of vibronic bands and the modeling of Franck-Condon integrals. Qualitative considerations on geometry changes based on the intensity of vibronic bands are very popular in photochemistry and spectroscopy. Modeling of the vibrational structure of UV-vis spectra based on the results of quantum-chemical calculations is also known in the literature, within various models of Franck-Condon factors and/or Herzberg-Teller vibronic coupling[0-3].

Unfortunately, quantitative estimation of the changes in the geometry of polyatomic molecules, based on the intensity of vibronic bands in the experimental spectra, is a difficult task that are undertaken rather rarely[4,5]. The difficulty of such experimental studies is related to the necessity of obtaining UV-vis spectra of polyatomic molecules with well resolved vibrational structure. This is achievable for molecules cooled to cryogenic temperatures and isolated from intermolecular interactions under supersonic-jet conditions, or matrix isolation in solid noble gases. These investigations require high spectral resolution and sensitivity achievable with the use of laser spectroscopy techniques.

The determined geometry changes make it possible to calculate the geometry parameters of a molecule in the excited state, since the ground-state geometry is usually established with good accuracy, on the basis of crystallographic measurements, X-ray or electron diffraction or microwave spectroscopy and NMR spectroscopy methods, which, however, cannot be used for the examination of molecules in excited electronic states.

The difficulty of theoretical calculations for excited states is associated with the geometry optimization and calculation the normal modes of the molecule, using quantum chemistry methods that provide a correct and balanced description of the electronic structure of the excited state as well as the geometry and vibrational structure of the molecule in this state. This requires taking into account both the multi-configurational electronic wave function for the excited state as well as the static and dynamic correlation of electrons, which is also necessary for a correct description of the hydrogen bond.

### *II.2.3. IMPORTANCE AND APPLICATIONS OF ANTHRANILIC ACID*

Although anthranilic acid, like salicylic acid, was discovered in the mid-19th century, it was only at the end of the 20th century that the unique photophysical and photochemical properties of its molecules in the $S_1(\pi\rightarrow\pi^*)$ excited state were discovered. They enabled the use of molecules of this molecules as molecular probes for the study of protein systems[6,7] and as a UV filter in cosmetics, and its derivatives for the production of conductive polymers used, among others, in OLED luminescent diode matrices.

Since the beginning of the 20th century, anthranilic acid has been used on a large scale in the chemical industry, primarily as a substrate for the production of organic azo dyes (including some acid-base indicators), and for the production of saccharin, and later also pesticides, insecticides and metal corrosion inhibitors. It is also widely used in the food industry as a food preservative, and its esters are used as fragrances in the perfume and cosmetics industries.

Anthranilic acid derivatives, due to their similarity to salicylates, have pharmaceutical applications as an important group of non-steroidal anti-inflammatory drugs and non-opioid analgesics. They are also used for the production of sulfonamides and loop diuretics. The role of anthranilic acid in living organisms, as an important intermediate product in the process of tryptophan biosynthesis, was recognized in the second half of the 20th century. From tryptophan, which is an important amino acid, in the subsequent stages of biochemical transformations, many biomolecules are synthesized that have diverse biological effects, among them: serotonin, melatonin, vitamin $B_3$ (PP), and plant growth hormones – auxins. Anthranilic acid is also an important component of dyes found in the lens of the eye.

Due to their unique photochemical properties, anthranilic acid molecules are used as molecular fluorescence probes in the process of fluorescence resonance energy transfer[6,7] FRET. High fluorescence yield, convenient spectral range in near-UV and relatively small molecular size facilitate the use of this compound as a efficient fluorescent probe. The fluorescent properties of anthranilic acid depends not only on the polarity of the environment but also on the amino acid to which its molecule is bound. Especially when it is bound to proline or tryptophan, the quantum yield of fluorescence decreases by an order of magnitude, but the mechanism of this phenomenon is not yet fully understood.

### *II.2.4. THE EXCITED-STATE INTRAMOLECULAR PROTON TRANSFER ESIPT VERSUS PHOTOPHISICAL AND PHOTOCHEMICAL PROPERTIES OF ANTHRANILIC ACID*

The electronic excitation in molecules forming an intramolecular hydrogen bond that involves functional groups coupled to the π-electronic system, usually causes a pronounced strengthening of the hydrogen bond. It often manifests itself through the phenomena listed below.

1. The presence of a strongly red-shifted dual fluorescence band (in methyl salilcylate[8,9] molecules and other salicylic acid derivatives).
2. Significant shortening of the total length of the hydrogen bridge, reaching 0.3Å.
3. Noticeable displacement of a hydrogen atom on the hydrogen bond and lengthening of the O–H covalent bond in which it participates.
4. Drastic reduction in the frequency of the O–H stretching vibration that involves the hydrogen atom participating in the hydrogen bond (even by more than 1000 $\mathrm{cm}^{-1}$).

The dual fluorescence of methyl salicylate molecules was studied by Weller[8], who first proposed as their explanation the mechanism of intramolecular proton transfer in the excited state ESIPT. However, in-depth studies of salicylic acid derivatives by UV spectroscopy[9-12], Raman[13] and infrared[14] 14 spectroscopy indicated the essential role of vibrational relaxation, involving low-frequency skeletal vibrations in many of the investigated molecules. Also, femtosecond spectroscopy[15] studies have shown that the time scale of this process is characteristic for the displacement of skeletal atoms (second row atoms) rather than the light hydrogen atom. Also quantum-chemical calculations showed[16-19] that both the shortening of the total length of the hydrogen bridge, reaching about 0.3 Å, as well as the lengthening of the covalent O–H bond by 0.15Å, although quite significant, are, however, clearly smaller than required for the total proton transfer. Moreover, calculations have shown that the change of dipole moment upon the π-electronic excitation is usually small, thus the excited-state intramolecular hydrogen atom dislocation ESIHT occurs rather than the intramolecular proton transfer ESIPT. Although in many molecules, the mechanism of this phenomenon is more multi-faceted than the originally postulated ESIPT process, reference is usually made to ESIHT and ESIPT, although this interpretation is often simplified.

Anthranilic acid is one of the model molecule for the study of properties excited by aromatic molecules, in which functional groups coupled with the π-electronic system form the N–H···O=C intramolecular hydrogen bond. In the excited state, hyperconjugation of these substituents with the aromatic system causes significant strengthening of the hydrogen bond. Anthranilic acid is similar to salicylic acid and other α-hydroxyl derivatives of carbonyl compounds, in which the emission of the strongly stokes-shifted dual fluorescence is observed.

In the anthranilic acid molecule, the changes related to the strengthening of the hydrogen bond upon the excitation are similar in nature, but less intense than in salicylic acid derivatives, making it a convenient model molecule for analogous studies. Although anthranilic acid does not emit dual fluorescence, it is observed in the emission spectra of its derivatives, as well as its ammonium cation in the acidic environment at pH≈1, bound in the inclusion complex with β-cyclodextrin[20]. The anthranilic acid molecule is a model molecule for experimental studies on geometry changes, because it does not exhibit any significant interference with the Franck-Condon distribution for band intensities in the LIF spectrum of the $S_0 \rightarrow S_1$ transition. Geometry changes occur without the need to overcome an energy barrier, on a single potential energy surface[21] and there is no low-energy intersection of the π-π* and n-π* states, which in salicylic acid derivatives often causes relaxation to the ground state and fluorescence quenching[10,19].

However, analogous studies of anthranilic acid and its derivatives began much later than those of salicylic acid. The latest systematic study of absorption spectra and fluorescence of anthranilic acid in a series of solvents covering a wide range of polarities (dielectric constants) was carried in the 21st century[20]. The studies of anthranilic acid molecules and its dimer in supersonic molecular beam also began in the 21st century. They were conducted with various laser spectroscopy techniques in the group of Prof. Zwier[22-24], with the use of: LIF fluorescence excitation spectra, IR-UV hole burning spectroscopy, REMPI/TOF resonance enhanced multiphoton ionization time of flight mass spectrometry, as well as single vibronic level dispersed fluorescence spectra and IR-UV double resonance. Studies of spectra in supersonic molecular beams for *ortho*-, *meta*- and *para*-anthranilic acid isomers and their water complexes were carried out by Kong et al.[25-27]. Recently, spectroscopy, photophysics and ultrafast kinetics for excited-state relaxation of methyl anthranilate[28,29] have also attracted the attention of researchers due to its use as a UV filter.

Although the aforementioned experimental studies of the anthranilic acid molecule[22-25] provided a lot of information regarding the dynamics of the excited molecule, they did not provide quantitative structural information on excited-state geometry and the geometry changes upon the excitation. The only quantitative results concerning these came from quantum-chemical calculations using the TDDFT method of Prof. Sobolewski and Domke[21].

## II.3. RESEACH METHODS

In quantitative studies of changes in equilibrium geometry of anthranilic acid molecules, I used, in a complementary and synergistic way the techniques and methods listed below, which are part of three specialties: experimental and theoretical molecular spectroscopy and quantum chemistry,.

1. Advanced methods of high resolution spectroscopy: studies of laser-induced fluorescence LIF excitation spectra of molecules isolated from intermolecular interactions and cooled to cryogenic temperatures in supersonic molecular beam.
2. Modelling of multidimensional FC factors using methods of theoretical spectroscopy: in an advanced model taking into account also changes in frequencies of normal vibrations and the Dushinsky effect.
3. Quantum-chemical calculations for molecules in electronic excited states: using multi-configuration quantum chemistry methods, taking into account also dynamic correlation of electrons and adequate modelling of the hydrogen bond.

## *II.3.1. THE LASER-INDUCED FLUORESCENCE LIF EXCITATION SPECTRA IN THE SUPERSONIC MOLECULAR BEAM*

### *Supersonic molecular beam technique*

Only the spectra of molecules isolated from intermolecular interactions and cooled to cryogenic temperatures reveal a rich and well-resolved vibrational structure, which can provide extensive experimental information needed to determine the equilibrium geometry changes of polyatomic molecules. Due to the above requirements, I investigated the spectra of the anthranilic acid molecule and its isotopomers (isotopologues) under the conditions of the supersonic molecular beam, using the technique of pulsed supersonic free jet, with helium as a carrier gas, to minimize intermolecular interactions.

The supersonic molecular beam method is a unique technique that allows to obtain molecules cooled to cryogenic temperatures of a few kelvins. This method is also called supersonic expansion or supersonic jet technique. The supersonic expansion technique consists in a rapid expansion of the gas stream, from the pressure of several atmospheres to high vacuum ($p < 10\text{-}6$ atm), injected into the vacuum chamber through a narrow orifice called a nozzle. Almost without resistance, the gas stream undergoes a very rapid adiabatic expansion, causing its very rapid cooling. Then, in the kinetic region the stream expands further and is cooled down. During this process the energy of chaotic thermal motions of the molecules is converted into the kinetic energy of their systematic motion of a whole stream along the direction of the jet propagation. As a result, the velocity of the jet is many times higher than the velocity of the sound in such a diluted gas, reaching the Mach number even of several hundred. Very rapid expansion and cooling of the gas also leads to a significant increase in the average time between collisions, as a result it exceeds many times the lifetime of polyatomic molecules in excited electronic states. Therefore, the supersonic jet expansion generates molecules isolated from intermolecular interactions that are cooled to a translational temperature of 0.1 K and a rotational temperature of a few kelvin.

### *Laser-induced fluorescence LIF excitation spectra*

Spectroscopic measurements in such a diluted gas (under conditions corresponding to the molar concentration of the order of $10^{-12}$ mol/dm$^3$) require the use of advanced laser instrumentation and laser spectroscopy techniques which, in addition to high spectral resolution of the order of 0.1 cm$^{-1}$, also provide very high sensitivity of the detection of the weak fluorescence signal. Among such techniques is the measurement of laser-induced fluorescence excitation spectra (LIF). The use of advanced laser equipment guarantees resolving power of about 100 000 and instrumental spectral resolution of about $10^{-4}$ nm, in the ultraviolet range, which corresponds to about 0.1-0.2 cm$^{-1}$ in wavenumber and is comparable to the rotational constant of polyatomic molecules consisting of several atoms. As a result, the resolution of the LIF spectra for such molecules is not limited by the instrumental resolution, but only by the width of the rotational profile, resulting from fundamental physical relations.

The LIF spectra investigated in the period 2004-2010[H2,H4] I recorded using the equipment for the laser-induced fluorescence excitation spectra in supersonic molecular beams described in the paper[H2], located in the Department of Physical Chemistry and Electrochemistry at the Faculty of Chemistry of the Jagiellonian University(Poland). The later experiments (in the period 2013-2019) I carried out on a newly-constructed equipment for laser spectroscopy in supersonic molecular beams (described in Section III.1.2), located in the Centre for Innovation and Transfer of Natural Science and Engineering Knowledge of the University of Rzeszów (Poland) at the Faculty of Mathematics and Natural Sciences.

### *II.3.2. QUANTUM CHEMISTRY CALCULATIONS FOR MOLECULES IN EXCITED STATES*

For a correct and balanced description of the excited state $S_1(\pi \rightarrow \pi^*)$ dominated by the single-electron HOMO-LUMO excitation, calculations using multi-configurational quantum chemistry methods, taking into account all relevant single-excited configurations are required. In addition, to achieve high accuracy and for adequate modeling of hydrogen bonded systems, it is particularly important to take into account the dynamic electron correlation.

The geometry optimization and computational vibrational analysis (calculations of normal modes) for molecules in the excited electronic state were performed using the quantum chemistry methods listed below.

1. Initially, I performed calculations using the Configuration Interaction of Singly-excited configurations, CIS, SCI.
2. I performed calculations with TD-DFT(B3LYP) method for the molecule in excited state, as a widely used quantum chemistry method for single-electron excitations.
3. In order to achieve the quantum-chemistry results of optimal quality and relevance for the experimental data, I performed calculations using the approximate perturbative coupled cluster method CC2[30-32].

In the earlier works[H1,H2], quantum chemistry calculations using the HF and CIS methods were performed with Pople's basis sets: 6-31G** and 6-31+G**. In the later works[H3-H7], calculations using the DFT and CC2 methods were performed with a series of Dunning correlation consistent basis sets: cc-pVXZ(X=D,T,Q) and aug-cc-pVXZ(X=D,T).

### *II.3.1. MODELING FRANCK-CONDON FACTORS AND MODELING OF THE CHANGES IN THE EQUILIBRIUM MOLECULAR GEOMETRY BASED ON THE EXPERIMENTAL INTENSITIES OF VIBRONIC BANDS*

For the investigated electronic transition, the relative intensities of the vibronic bands, given by the FC factors, are determined primarily by the differences in the equilibrium geometry between the ground state and the excited state. Therefore, preliminary analyses of experimental band intensities and modeling of FC factors were performed in a 1-dimensional model, based on the displaced harmonic oscillator model (DHO).

In order to obtain the highest possible accuracy and reliability of the results, I have performed calculations of band intensities in the multidimensional model of FC factors, that takes into account not only the influence of changes in the equilibrium geometry of the molecule, but also the influence of changes in vibration frequency and the Dushinsky effect, associated with the so-called "mode mixing". The modeling of band intensities in the studied LIF spectra was carried out[H1,H3,H7] using matrix recursive equations for the calculation of multidimensional FC factors in Cartesian coordinates, derived by Doktorov[33], and using the effective computational algorithms developed by Gruner[34] and Ruhoff[35,36].

Since the underestimation of modeled band intensities results from too small values of geometry changes, calculated by quantum chemistry methods, I carried out the least-square fitting of displacement parameters iteratively, for normal coordinates, in order to obtain optimal agreement with experimental band intensities[H3,H7]. Subsequently, on the basis of the experimentally-based values of the reduced displacement parameters and the normal modes computed with quantum chemistry calculations, I determined the differences in equilibrium geometry of the molecule, between the ground and the excited state.

## II.4. RESEARCH AND RESULTS

Modeling of Franck-Condon factors in multidimensional modelH1 was carried out on the basis of the results of ab initio quantum-chemistry calculations for the $S_0 \rightarrow S_1(\pi\text{-}\pi^*)$ transitions in anthranilic acid, methyl anthranilate, salicylic acid and anthranilonitriles. (It should be mentioned that the author's PhD dissertation on the LIF spectra of anthranilonitriles did not include the modeling of FC factors, neither for the modeling of band intensities in the spectra LIF spectra nor for modeling of changes in geometry, whereas the H1 publication does not include any experimental studies but only quantum-chemistry calculations and theoretical modeling of FC factors.)

Since the investigated excited states of $S_1$ for the molecules under consideration are dominated by the HOMO-LUMO excitation, the basic adequate level of ab initio calculations is the CIS method for the excited state and the Hartree-Fock method for the ground state. These modeling have shown significant values of FC factors mainly for the in-plane rocking vibrations of the substituents and, to a lesser extent, for the bending vibrations of the aromatic ring. Moreover, they showed that in the experimental spectra, high intensity of bands associated with rocking vibrations of the substituents occurs for the *ortho-* substituted isomers. However, the above fact is only partially reflected in the band intensities calculated by the FC modeling on the basis of quantum-chemistry calculations, which is particularly pronounced for the molecules with the intramolecular hydrogen bonding between substituents, such as in salicylic acid, anthranilic acid and methyl anthranilate.

### *II.4.1 STUDIES OF LIF EXCITATION SPECTRA OF MOLECULES COOLED IN SUPERSONIC JET EXPANSION*

The LIF spectra studied in the years 2004-2010[H2,H4] were recorded on an apparatus for measuring spectra of laser-induced fluorescence in supersonic molecular beams, located in the Department of Physical Chemistry and Electrochemistry at the Faculty of Chemistry of the Jagiellonian University. The LIF spectra of deuterated molecules with various isotopic exchange ratio[H5] and more accurate measurements of relative intensities for vibronic bands in the LIF spectrum of anthranilic acid[H7] were recorded in 2013-2019 on a newly constructed apparatus for laser spectroscopy in supersonic molecular beams (described in Section III.1.2), built by me as part of the Molecular Spectroscopy Laboratory, at the Centre for Innovation and Transfer of Technical and Natural Knowledge at the Faculty of Mathematics and Natural Sciences of the University of Rzeszów.

As the subject of further research, aimed at obtaining a consistent and quantitatively adequate modeling of equilibrium geometry changes due to excitation, I chose the anthranilic acid molecule. In the laser induced fluorescence excitation spectra LIF of anthranilic acid, I observed from several dozen to over a hundred vibronic bands[H2,H4,H5] within the investigated electronic transition band. It was achieved by optimizing the experimental conditions, the reduction of scattering of the laser beam, improving rotational cooling and minimizing saturation effects. Owing to the above, the spectral bandwidth of rotational profiles reduced to approximately 1.5-1.7 $\mathrm{cm}^{-1}$ was achieved for most of vibroinic bands, i.e. 2-3 times smaller value than in previously published spectra[22-25]. Such widths of rotational profiles in the spectra of the investigated molecule correspond to the rotational temperature $T_{\mathrm{rot}} \approx 0.3\text{-}0.5$ K, compared to Trot≈2-3K obtained in the previously published studies[22-25]. Owing to the above I obtained better separation of vibronic bands improved in comparison with those typically obtained in supersonic molecular beams. This resulted in a much larger pool of spectral data (listed and analyzed in [H2], and for deuterated molecules in [H4, H5]). On the basis of these data, I detected over 100 vibronic bands in the LIF spectrum and the activity of 10 totally-symmetric normal modes (compared to only four identified in previous studies[22,25]).

In order to correctly determine the relative intensities of vibronic bands in the LIF spectra, I applied normalization of the fluorescence signal, by dividing its value by the intensity of the excitation beam[H2,H4,H5,H7]. Such normalization of the signal ensures elimination of the influence of both: fluctuations of the energy of the laser beam (up to about 30%) and several times larger systematic changes of its intensity.

### *Distinction between the vibronic bands of monomer and dimer*

An important complication in the study of isolated carboxylic acid molecules is their strong tendency to form dimers, owing to the presence of hydrogen bonds between the carboxylic groups of both molecules. The distinction of vibronic bands belonging to spectrally overlapping electronic transitions of monomer and dimer was done in two ways[H2].

1) By analyzing the progression and combinational transitions present in both spectra, in particular the progression of low frequency (57 cm$^{-1}$) intermolecular vibration, which is characteristic of the dimer (bands marked with an asterisk in Fig.1);
2) By adjusting the experimental conditions in such a way that systematic differences in intensity between the monomer and dimer bands are displayed in a series of spectra.

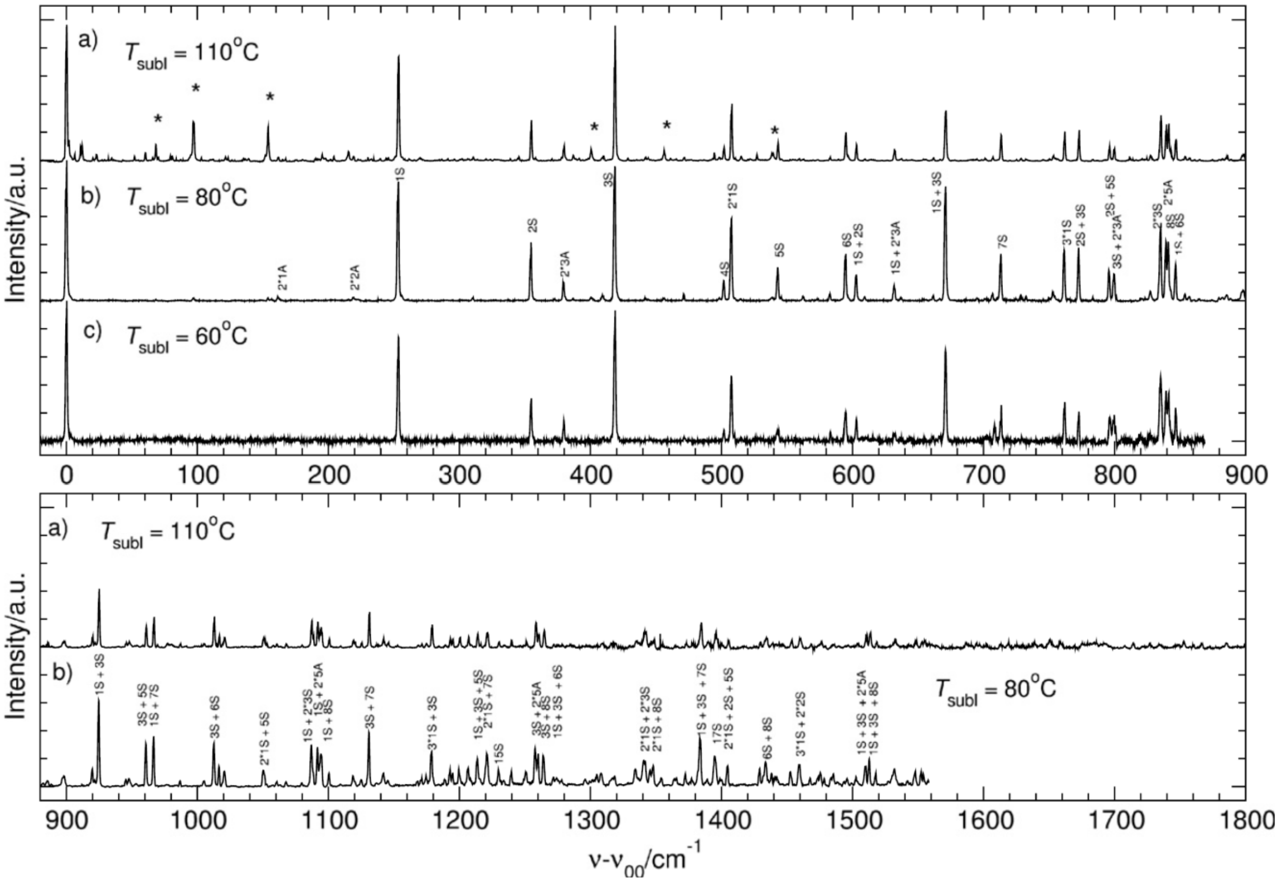

**Fig. 1.** [H2] LIF spectra of anthranilic acid recorded at w at various sublimation temperatures of the solid sample (for various vapour pressure of anthranilic acid). In order to enhance vibrational analysis of the spectra, the wavelength for adiabatic transition ($\nu_{00}$ = 28591 cm$^{-1}$) is subtracted from the value on the horizontal axis. The dimer bands are marked with an asterisk. Symbols 1S,...8S denote totally-symmetric normal modes, numbered according to increasing frequency.

The latter was made possible by using a roughly quadratic dependence of the concentration of the dimer in the gaseous phase on the vapour pressure of anthranilic acid, which increases with the sublimation temperature of the sample. Thus, in the spectra recorded at low sublimation temperatures, the bands coming from the dimer were almost completely eliminated from the gas-phase spectra, and at 80$^0$C the advantageous properties of the recorded spectrum were preserved: a relatively strong signal coming from the monomer spectrum and high signal-to-noise ratio (Fig.1). The distinction between the monomer and dimer spectra, achieved by UV-vis spectroscopy techniques with the detection based on ionization and mass selection of created molecular ions, was described earlier in the literature. Such studies were carried out with hole-burning spectroscopy as well as resonantly enhanced multiphoton ionization techniques REMPI, combined with time of flight mass selection TOF (REMPI/TOF spectra[22,23]. However, the application of these techniques in my research was impossible because it would require an extensive and very costly upgrade and reconstruction of the experimental setup. Moreover, much better band separation and higher signal-to-noise ratio were achieved in the LIF spectra[H2] than in REMPI/TOF spectrum of anthranilic acid the published elsewhere[22,23].

### *Franck-Condon simulation of band intensities based on the experimental data*

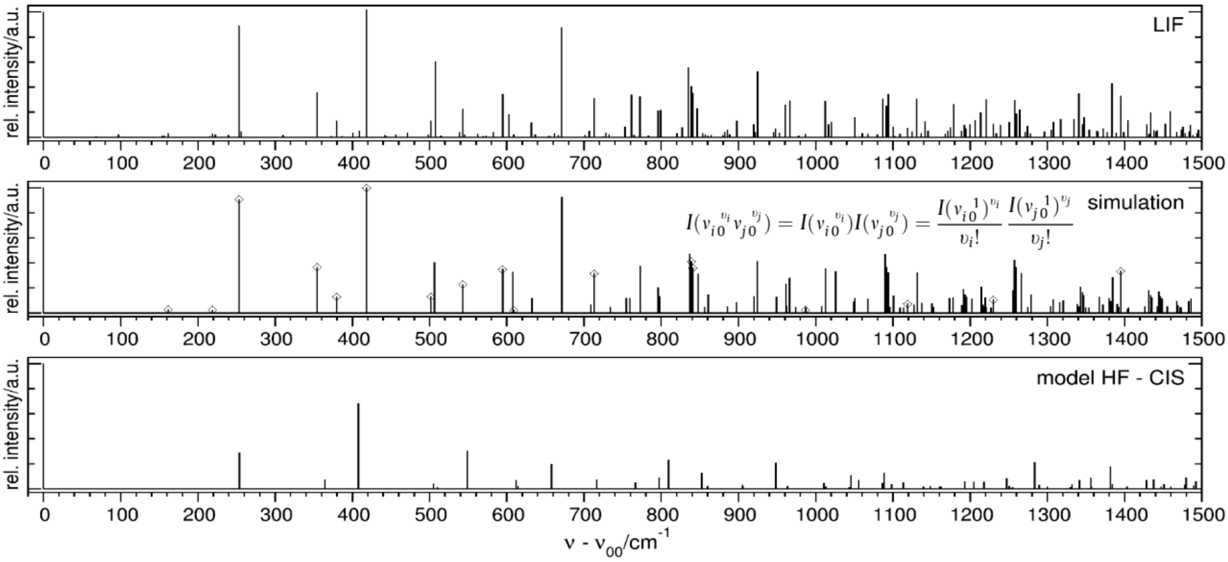

**Fig. 2.** [H2] Comparison of experimental intensities in the LIF spectrum (upper spectrum); and values modeled on the basis of the intensities of fundamental transitions (symbol ○) for $\upsilon = 0 \rightarrow \upsilon = 1$ (middle spectrum); and intensities calculated on the basis of quantum-chemical calculations using CIS and Hartree-Fock method in the model of one-dimensional FC factors (lower spectrum).

The obtained LIF spectra provided a good starting point for the Franck-Condon analysis, when earlier attempts mentioned in the literature were unsuccessful[22]. The analysis of intensities in the experimental spectra (upper spectrum in Fig.2) confirmed the Franc-Condon distribution of band intensities[H2] and the dominant influence of displacement parameters for particular vibrations on this distribution, with negligible influence of other factors (such as Dushinsky effect or Fermi resonance). This is demonstrated by the simulation of the Franck-Condon distribution of band intensities based on fundamental transitions $\upsilon = 0 \rightarrow 1$, presented as the middle spectrum in Fig.2, which shows very good agreement with the intensities in the experimental spectrum. Similar analyses were carried out for isotopomers deuterated in functional groups[H4,H5]. As a result of the intensity analysis, relative integral band intensities were determined, as well as the experimental values of the reduced displacement parameters for individual normal vibrations. These values provided the ground for determining the experimentally-based values of the changes in equilibrium geometry of the anthranilic acid molecule upon the excitation[H3,H7].

On the other hand, band intensities modeled using the values of dimensionless displacement parameters, calculated on the basis of the results of quantum-chemistry calculations with the CIS method for the excited state and Hartree-Fock for the ground state (lower spectrum in Figure 2) are drastically underestimated. The comparison with the simulation described above, carried out according to the same model on the basis of experimental results, shows unequivocally that the underestimated change in the equilibrium geometry between both states, calculated by these methods that is the root of this discrepancy. Therefore, in order to improve this deficiency of the HF and CIS results, it is necessary to use more advanced methods of quantum chemistry, which are discussed in the section on quantum-chemical calculations (Sect. II.4.4).

### *II.4.2 ANHARMONICITY OF MOLECULAR VIBRATIONS*

Antharmonic effects are another important issue that was investigated owing to the improvement in accuracy of the determination of frequencies for vibronic bands. Narrow rotational profiles made possible the determination of the center of vibronic bands (defined as so-called "center of the mass") with the accuracy of about 0.2 cm$^{-1}$. Owing to the above it was possible to observe anharmonic effects, occurring in the two most important progressions of the studied spectrumH2,H4 ($\nu_{1S} = 253\ \mathrm{cm}^{-1}$ i $\nu_{3S} = 419\ \mathrm{cm}^{-1}$).

The detection of this small anharmonism (characterized by diagonal anharmonic parameters of the order of tenths of an reciprocal centimeter[H2]) is quite rarely achieved in studies vibrational structure of UV spectra for polyatomic molecules of this size. Nevertheless, the determination of even small anharmonic parameters for the most important normal vibrations active in the LIF spectrum, resulted in corrections of magnitude ±10 cm$^{-1}$, which often changed the assignments for further bands in progressions ($\Delta\upsilon$ = 2.3.4, etc.) and complex combination transitions, that had previously been reported in the literature. This had a significant effect on the results of the Franck-Condon analysis and on the determined changes in the equilibrium geometry of the molecule. The magnitude of anharmonic corrections in the studied progressions was compared with the results of anharmonic vibrational calculations using CIS[H2] method. An analogous analysis was performed for isotopomer deuterated in the functional groups ($ND_2$, COOD)[H3].

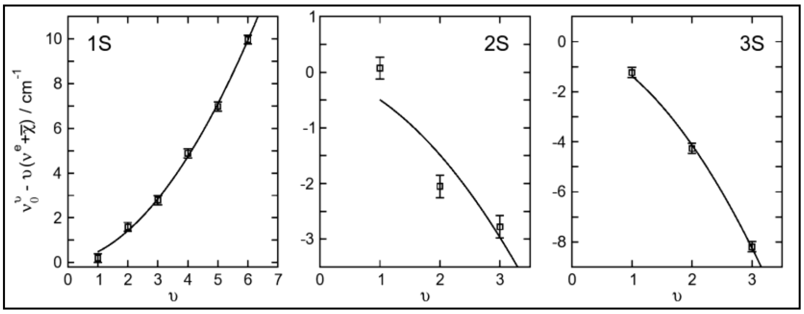

**Fig. 3.** [H2] Fitting of the first anharmonic correction to the positions of bands in the progressions of the following vibrations: $\nu_{1S} = 253\ \mathrm{cm}^{-1}$, $\nu_{2S} = 354\ \mathrm{cm}^{-1}$ i$\nu_{3S} = 419\ \mathrm{cm}^{-1}$. On the horizontal axis vibrational quantum number is marked for transitions in progressions. On the vertical axis the deviations from harmonic frequencies are shown. The continuous curve lines mark the fragments of parabolas that give the best fit of anharmonic parameters.

### *II.4.3 ISOTOPIC EFFECTS AND THEIR IMPLICATIONS FOR THE MOLECUALR DYNAMICS*

The interpretation of the observed bands and the activity of totally-symmetric oscillations were confirmed on the basis of the studies of isotopic effects in the spectra of molecules deuterated in function groups[H4,H5]. The most complex of these spectra contained eight ($2^3$) overlapping spectra belonging to the molecules containing from one to three deuterium atoms substituted in various positions in the $NH_2$ and COOH groups (Fig. 4)[H5].

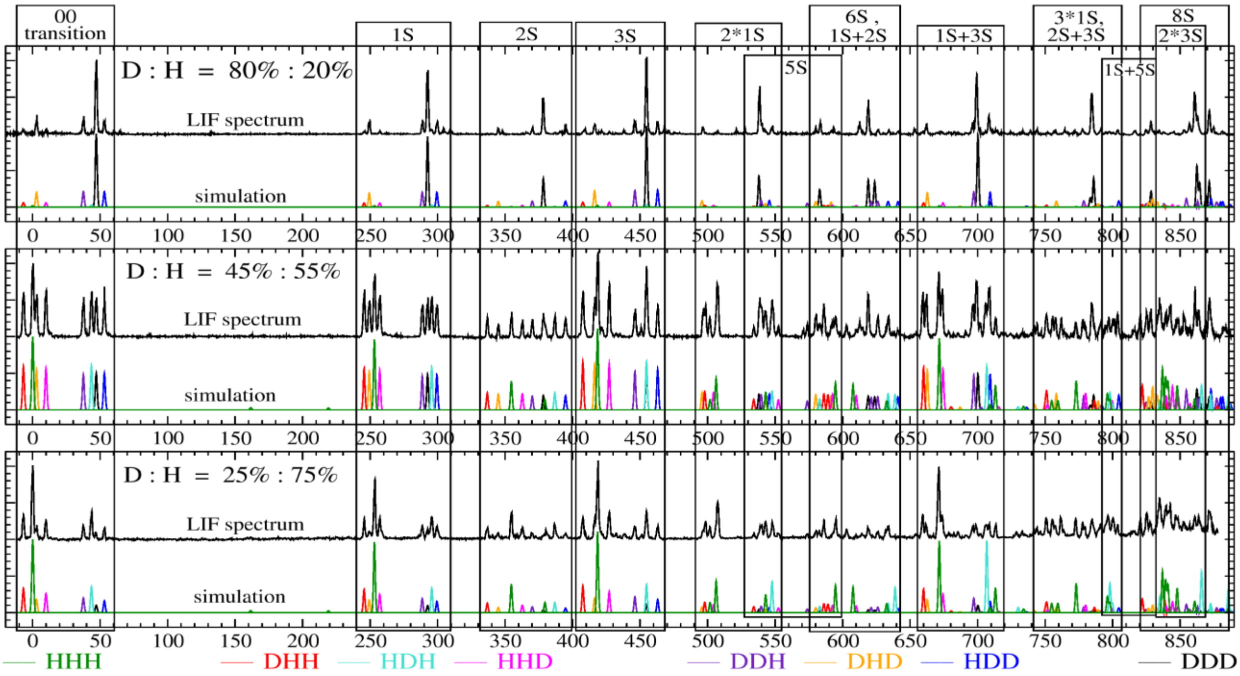

**Fig. 4.** [H5]. LIF spectra of samples of anthranilic acid partly deuterated in the substiuent groups: NH$_2$ and COOH. The wavelength of the adiabatic transition $v_{00}$ = 28591 cm$^{-1}$ for the non-deuterated isotopologue HHH is subtracted from the value shown on the horizontal axis. Below each spectrum the spectrum simulated on the basis of frequencies and intensities of fundamental transitions for eight isotopomers is presented. Isotopomers are denoted by the presence of H or D atoms in the positions 1, 2 and 3: H(1)-N-H(2)···O=C-OH(3).

The comparative analysis of these spectra and the analysis of progressions and combinational transitions present in the overlapping component spectra (analogous to the work [H2]), allowed for separation of all eight component spectra, determination of the changes frequencies for the vibrations active in LIF spectra and the shifts of the adiabatic transition as a result of isotopic substitution[H5]. The unambiguous assignment of the eight component spectra to the specific isotopomers was established on the basis of the correlations between the experimental frequencies in the LIF spectra and the vibrational frequencies calculated using quantum chemistry methods, as they show a monotonic order (Fig. 5) for all the investigated vibrations[H5], except for the $v_{8S}$ vibration.

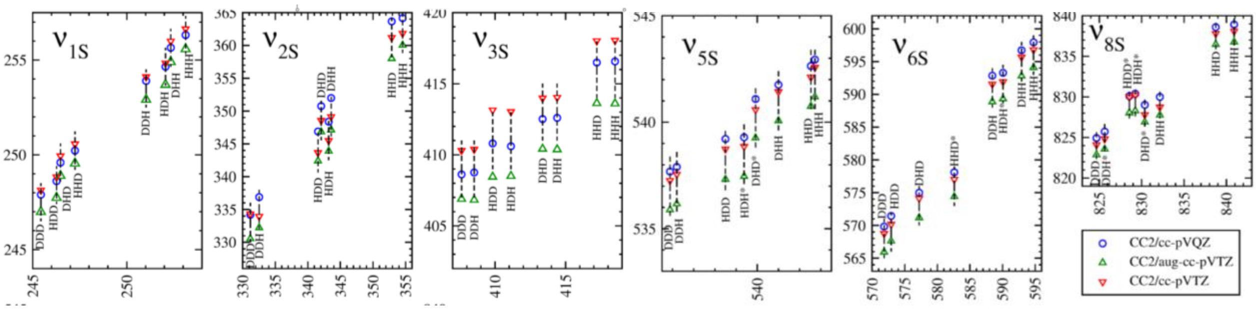

**Fig.5** [H5] Correlation of the isotopically-induced frequency shifts for normal modes active in the LIF spectra and computed with the CC2 coupled cluster method.

### *Isotopically-induced frequency changes as a function of Cartesian displacements of atoms in normal modes*

In order to quantitatively correlate the change in vibrational frequency with the amplitudes of motions for atoms subject to isotopic substitution without losing sight of simple physical interpretation I have derived a simple estimation of frequency changes. For the oscillations that retain their unchanged characteristics, I carried out the reasoning[H5] presented below. In the harmonic approximation, the frequency of a given vibration is proportional to the square root of the force constant divided by the reduced mass. If the characteristic of a given vibrational mode is retained only reduced mass change upon the isotopic substitution. For example, the ratio of the frequencies for a given oscillation for an unsubstituted isotopomer (denoted as HHH), and for an isotopomer substituted (e.g. containing three deuterium atoms in functional groups ND2, COOD, denoted as DDD), is given by Eq. (1).

$$\frac{\nu_{\mathrm{DDD},i}}{\nu_{\mathrm{HHH},i}} = \sqrt{\frac{\mu_{\mathrm{HHH},i}}{\mu_{\mathrm{DDD},i}}} \tag{1}$$

Therefore, the problem of calculating the above frequency ratio reduces to the problem of calculating the ratio reduced masses for the considered vibration in both isotopomers.

In order to calculate the reduced masses for vibrations, I used Cartesian displacements of atoms from equilibrium positions, normalized according to Eq. (2), describing the vectors normal modes and grouped in columns of the $\mathbf{L}^{\mathrm{Cart}}$ matrix.

$$|\vec{Q}^{\mathrm{Cart}}_{\mathrm{norm},i}|^2 = \sum_k^{3N} \Delta x_{\mathrm{norm},}{}^2_{ki} = \sum_k^{3N} L^{\mathrm{Cart},\ 2}_{\mathrm{norm},ki} = 1 \tag{2}$$

As a consequence, the displacements of the *k*-th atom in the *i*-th normal vibration in the mass weighted coordinates ( $\xi_{ki} = x_{ki}\sqrt{m_k}$ ), which can be grouped in a $\mathbf{L}^{\mathrm{MW}}$ matrix are normalized to the square root of the reduced mass for this vibration, according to Eq.(3).

$$|\vec{Q}^{\mathrm{MW}}_i|^2 = \sum_k^{3N} \Delta\xi^2_{ki} = \sum_k^{3N} L^{\mathrm{MW},2}_{ki} = \mu_i \tag{3}$$

This normalization gives directly contributions of the mass for individual atoms in the reduced mass of a given vibration. The reduced mass of the vibration can be treated as the weighted average of atomic masses, with the weights equal to the squares of the normalized Cartesian amplitudes atoms. Thus, the reduced mass of each normal vibration can be decomposed into the sum of the contributions for the atoms subject to isotopic substitutions and the sum of contributions for other atoms. In these expressions the squares of weighted coordinates could be represented by squares of Cartesian coordinates multiplied by the atomic masses. For the non-substituted isomer (HHH) and the deuterated isomer containing three D atoms in functional groups (DDD), these expressions take the form given by Eq.(4).

$$\mu_{\mathrm{HHH},i} = \sum_k^{3N-iso} L^{\mathrm{MW},\ 2}_{\mathrm{HHH},ik} + \sum_k^{iso} L^{\mathrm{MW},\ 2}_{\mathrm{HHH},ik} = \sum_k^{3N-iso} \Delta x^2_{\mathrm{HHH,norm},ik} m_k + m_{\mathrm{H}} \sum_k^{iso} \Delta x^2_{\mathrm{HHH,norm},ik}$$

$$\mu_{\mathrm{DDD},i} = \sum_k^{3N-iso} L^{\mathrm{MW},\ 2}_{\mathrm{DDD},ik} + \sum_k^{iso} L^{\mathrm{MW},\ 2}_{\mathrm{DDD},ik} = \sum_k^{3N-iso} \Delta x^2_{\mathrm{DDD,norm},ik} m_k + m_{\mathrm{D}} \sum_k^{iso} \Delta x^2_{\mathrm{DDD,norm},ik} \tag{4}$$

Comparing the two expressions leads to an expression for the reduced mass for vibration of the deuterated molecule, containing the reduced mass for this vibration in the unsubstituted molecule and the difference of masses for both isotopes multiplied by the sum of squares of Cartesian amplitudes for atoms subject to isotopic substitution Eq. (5).

$$\mu_{\mathrm{DDD},i} = \mu_{\mathrm{HHH},i} + (m_{\mathrm{D}} - m_{\mathrm{H}}) \sum_k^{\mathrm{iso}} \Delta x^2_{\mathrm{HHH,norm},ki} \tag{5}$$

The substitution of the above expression (Eq.4) into Eq (1), finally gives the equation the for the frequency ratio of the considered oscillation as a function of the reduced mass of the considered vibration before isotopic replacement and the sum of the squares of Cartesian displacements of the atoms subject to isotopic substitution Eq.(6).

$$\frac{\nu_{\mathrm{DDD},i}}{\nu_{\mathrm{HHH},i}} = f\left(\mu_i, \sum_k^{iso} \Delta x^2_{\mathrm{norm},ik}\right) = \sqrt{\frac{\mu_{\mathrm{HHH},i}}{\mu_{\mathrm{HHH},i} + (m_\mathrm{D} - m_\mathrm{H}) \sum_k^{iso} \Delta x^2_{\mathrm{norm},ik}}} \qquad (6)$$

I verified this relation both on the basis of vibration frequencies calculated by quantum chemistry methods, as well as on the basis of extensive experimental data (frequencies of 6 normal vibrations for each of 8 isotopomers). Graphical representation of the above dependence based on the results of CC2/aug-ccpVTZ calculation for the vibrations active in LIF spectra (Fig. 6) shows that for the analyzed vibrations this dependence is fulfilled with good accuracy, however some deviations from it are noticeable for 3S, 6S and 8S vibrations.

The reasons of noticeable deviations of the relevant relations from the unit slope for some of the analyzed vibrations, both in case of comparison of frequencies calculated by quantum chemistry methods and experimental frequencies (Fig. 5), as well as the dependence of frequency ratio from displacements of atoms (Fig. 6), may result from two reasons. Firstly, form the inaccurate prediction of amplitudes of motions of hydrogen atoms that are subject to isotopic exchange. Thus, the underestimated slope in Fig. 5 and Fig. 6 for 3S, 5S and 8S vibrations may result from the underestimated amplitude of motions of the exchanged atoms, in vibrations calculated by quantum chemistry methods.

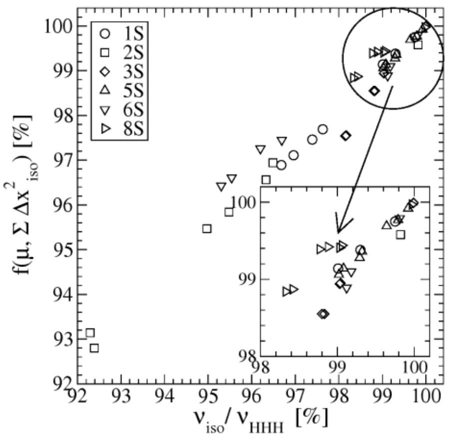

Fig. 6 [H5] The frequency ratio of the selected oscillations for the investigated deuterium substitutions versus the approximate ratio based on the Cartesian displacements of the substituted atoms. All values based on the CC2/aug-ccpVTZ ab initio results.

### *Inter-isotopic mode mixing*

The second reason for the deviations from the unit slope of the graphs (Fig.5 and Fig.6) results from the fact that the above simple relation (Eq. 6) is valid for molecular vibrations treated as independent oscillators. However, the strict solution of normal vibrations for isotopically substituted molecules (within Born-Oppenheimer approximation) requires simultaneous diagonalization of the kinematic matrix and the Hessian matrix (matrix of the second-order partial derivatives of potential energy), separately for both isotopically substituted molecules. Although Hessian of both molecules is identical, the kinematic matrices of both molecules are different, which lead to a characteristics of individual normal modes, which can be significant for some vibrations. The differences in mode pattern can be evaluated using the orthogonal transformation, analogous to the Dushinsky matrix.

In order to check the conditions of applicability of the proposed approximation (given in Equation 6) and to introduce a exact quantitative measure of the similarity of normal vibrations between molecules with different isotopic substitutions, I introduced a matrix describing the transformation of normal vibrations vectors between such molecules. Because for both( for the un-substituted and for the deuterated molecules) vectors of normal modes are orthogonal, the transformation between them is orthogonal. This transformation for the normal vectors normalized to unity in mass-weighted coordinates is expressed by the orthogonal matrix **R**. For example, the matrix for the transformation between the unsubstituted HHH isotopomer and for the isotopomer deuterated completely in functional groups DDD is defined Eq.(7).

$$\mathbf{R}_{\mathrm{HHH} \leftarrow \mathrm{DDD}} = \mathbf{L}^{\mathrm{MW,T}}_{\mathrm{norm,HHH}} \mathbf{L}^{\mathrm{MW}}_{\mathrm{norm,DDD}} \qquad (7)$$

The R matrix is an analogue of the Dushinsky matrix, whose elements are equal to the projections of normal mode vectors of a molecule in one electronic state, to the normal mode vectors of the molecule in the other electron state. The elements of the $\mathbf{R}_{\mathrm{HHH}\leftarrow\mathrm{DDD}}$ matrix, provide values of projections of appropriate normal mode vectors of the DDD isotopeomer to the HHH isomer and vice versa. Since squares of elements of the orthogonal matrix sum up to one in each column and in each row of the matrix, these elements are a strict and quantitative measure of the contribution of normal mode vectors of one isotopeomer to the normal mode vectors of another one.

Graphical representation of the squares of the matrix elements RHHH←DDD, being the values of the contributions of normal mode vectors of HHH isotopomer to the vibrations of DDD isotopomer (and each other) are shown in Fig. 7. The presence of a single large element non-diagonal position, in a given row or column, is related to large changes in vibrational frequency upon deuteration, which causes the change in numbering (vibrations of both molecules are automatically numbered according to the increasing frequency). On the other hand, the presence of several elements significantly different from zero in a given row or column, indicates the lack of unambiguous mapping of vibrations of both isotopomers. This effect can be called mixing of normal vibrations due to isotopic substitution or inter-isotopic mode mixing.

The vibrations in active the LIF spectrum (marked in Fig. 7 with symbols and arrows) undergo only small changes in their characteristics, measured by the square of the maximum matrix element, which is not less than 0.88 and for some of these vibrations this value reaches 98-99%. For the investigated vibrations, the small influence of inter-isotopic mode mixing, justifies why the estimation of changes in vibrational frequencies calculated basis of the amplitude of motions of the exchanged hydrogen atoms (in the approximation of independent vibrations), so well reflects the actual changes in frequencies. On the other hand, the inter-isotopic mode mixing occurs in the middle-frequency range (from 900 to 2000 cm$^{-1}$) and for out-off-plane vibrations.

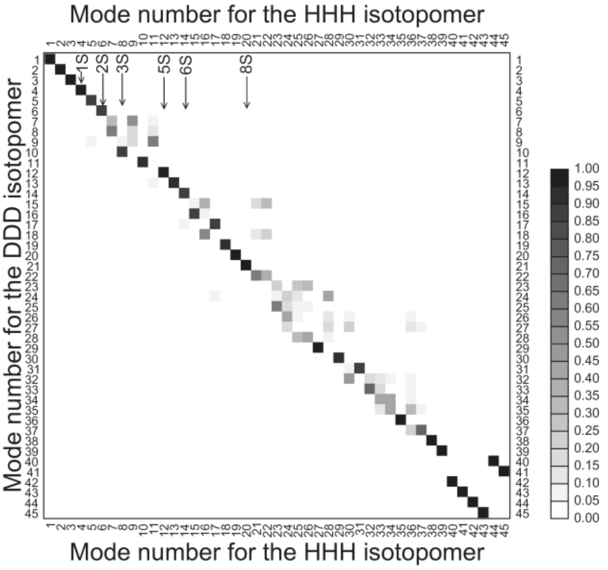

**Fig. 7** [H5] Squares of the element of the $\mathbf{R}_{\mathrm{HHH}\leftarrow\mathrm{DDD}}$ matrix computed on the basis of the CC2/aug-ccpVTZ vibrational analysis. Vibrations of both molecules are numbered according to the increasing frequency.

### *Implications of isotopic shifts of the adiabatic transition for molecular dynamics*

The shifts of the adiabatic transition in the $S_0 \rightarrow S_1$ spectrum of anthranilic acid[H5] (Fig. 8, left-hand diagram) were determined owing to the identification of the spectra of all eight investigated isotopomers. Additional verification of these assignments was obtained by comparing the isotopic shifts of the adiabatic transition for anthranilic acid and methyl anthranilate (Fig. 8, graph right), in which the methyl group replaces the hydrogen atom from the carboxyl group.

The shifts of the adiabatic transition result from the values of double differences of the energy of the zero vibrational level ΔΔZPE (zero point energy ZPE) between the ground and excited state, and simultaneously, between individual isotopomers of the molecule. In the anthranilic acid molecule, the shifts resulting from isotopic substitution of hydrogen atoms in particular positions in the functional groups are approximately additive[H5]. The largest contribution to the shift of adiabatic transition (about 47 cm$^{-1}$) is caused by the deuterium substitution of the hydrogen atom involved in the hydrogen bond[H5], whereas the exchange of all hydrogen atoms in functional groups ($ND_2$, COOD, in the isotopologue DDD[H2]) results in the shift of about 49 cm$^{-1}$.

So large value of the shift is caused by a drastic decrease of the N–H stretching frequency for the hydrogen atom involved in the intramolecular hydrogen bond in the excited state, which in case of deuteration in this position results in large changes of ZPE[H2]. This vibration was detected via IR-UV double resonance spectroscopy, FDIR (Fluorescence-Dip Infrared Spectroscopy)[22] at a frequency of 2900 cm$^{-1}$. Such a significant decrease of the $\nu_{N\text{–}H}$ frequency results from the strengthening the hydrogen bond, which causes weakening of the N–H bond[22].

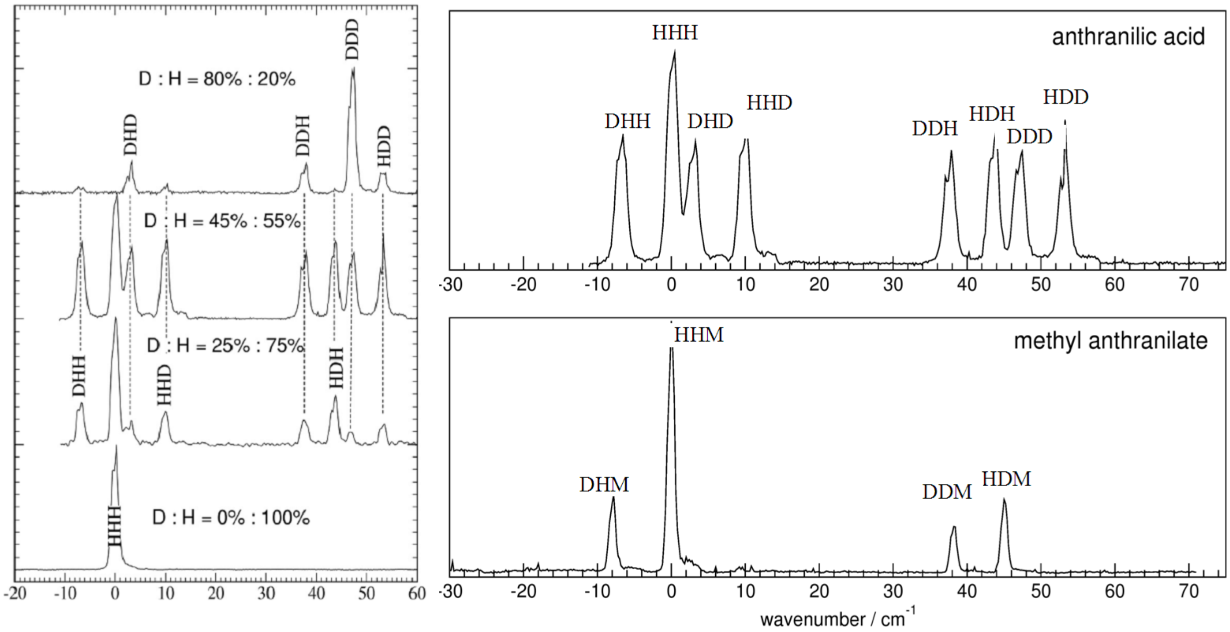

**Fig.8** [H5] Isotopic shifts of adiabatic transitions of anthranilic acid and methyl anthranilate. The assignments of anthranilic acid isotopomers denote H or D atoms in positions 1, 2 and 3: H(1)–N–H(2)···O=C–OH(3), and in methyl anthranilate HHM means: H(1)–N–H(2)···O=C–$OCH_3$(3). The wave number of the adiabatic transition for the undeuterated isotope (HHH for anthranilic acid and HHM for methyl anthranilate) was subtracted from the wave number on the horizontal axis.

Important information on the dynamics of the anthranilic acid molecule was established on the basis of studies of deuteration shifts for the adiabatic transition[H5] for all isotopomers. These shifts calculated as the double differences of the ab initio computed zero energy level of the ΔΔZPE for oscillations in the harmonic approximation shows considerable discrepancies with the experimental values. This is due to the fact that the equilibrium geometry of the anthranilic acid molecule in the ground state is not planar due to the non-planar amino group. In order to correctly calculate ZPE in deuterated isotopomers anthranilic acid, MP2, CC2, CCSD and CCSD (T) methods were used for the calculation of the potential energy curve and the energetic barrier for the inversion of the amino group. The barrier height was estimated[37] at about 40-55 cm$^{-1}$. The subsequent modeling of the ZPE the resulting double-well potential for oscillations having a significant contribution of the amino group inversion showed that the anthranilic acid molecule is dynamic planar[37], because the ZPE level for inversion of the amino group is about twice as high as barrier energy for the planar geometry. These calculations led to good agreement between the experimental and modeled shift adiabatic transition in the spectra of deuterated isotopomers of anthranilic acid. Thus, it was established that the anthranilic acid molecule is dynamically planar already in the ground state[37], due to the consistency between the experimental data and the results obtained on the basis of quantum-chemical calculations and the theoretical modeling of ZPE in the double-well potential. The above, together with the fact that the equilibrium geometry of the molecule in the excited state is planar, explains the low activity of off-plane vibrations in the LIF spectra, in which only a few even overtones for even values of vibrational quantum number were observed[H2].

### *II.4.4. QUANTUM CHEMISTRY CALCULATIONS USING THE HF, CIS, DFT, TDDFT AND CC2 METHODS FOR THE MOLECULE IN THE GROUND AND IN THE EXCITED STATE*

The choice of quantum chemistry methods used was determined by the following criteria. Primarily, for the relevant description of the $S_1(\pi\rightarrow\pi^*)$ excited state, dominated by the one-electron HOMO-LUMO excitation, taking into account the singly-excited configurations is sufficient. Moreover, to achieve high accuracy and adequate modeling of hydrogen-bonded systems it is particularly important to take into account the dynamic electron correlation. Additionally, for correct modeling of FC factor based on the difference between the equilibrium geometries of the ground and the excites electronic states, calculated using ab initio methods it is very important to maintain a consistent level of quantum chemistry methods used, both for electronic states of, and to perform calculations in the same basis set.

Calculations of geometry optimization and normal vibrations for the anthranilic acid molecule in the excited electronic state were made using the quantum chemistry methods listed below.

1. Initially, calculations were performed using the Configuration Interaction of Singly-excited configurations (CIS, SCI), which is the basic method allowing for a correct description of the electronic structure of the molecule in the investigated excited state, and using Hartee-Fock method for the ground electronic state. These methods, however, do not take into account electronic correlation but only interaction between electrons with in the averaged field model. In the [H1,H2] I made HF and CIS calculations for the anthranilic acid molecule. The aim of applying HF and CIS methods was to test the accuracy of predictions of these methods for a wide group of molecules[H1] and the relevance of the FC factors for anthranilic acid in the one-dimensional model[H2]. In the article[H3], the aim was to check to what extent the fitting of FC factors to the experimental data could compensate inaccuracy caused by the ab initio computed geometry changes and normal vibrations.
2. The TD-DFT(B3LYP) calculations were carried out for the molecule in excited state, because this is widely used quantum chemistry method for one-electron excitations. The calculations for the ground state were performed using DFT(B3LYP) method with the hybrid correlation-exchange function B3LYP. Density Functional Theory (DFT) takes into account electron correlation at relatively low computational cost. This method, combined with Time Dependent perturbation theory, facilitates relevant modeling of the states dominated by single excited configurations. Initially (in the work [H3]) I used the results of TD-DFT(B3LYP) calculations carried out by Prof. Andrzej Sobolewski, and in [H4] I used the results calculated by dr Marcin Andrzejak, computed using the Turbomole program. Due to the progress of computational programs and computer technologies, which significantly improved the availability of this method, in later works [H4-H7], I performed the TD-DFT calculations by myself using the Gaussian program.

3. In order to achieve the best available quality of quantum-chemical calculations and to be consistent with the experimental data, calculations were carried out using the CC2 coupled cluster method. CC2 is a perturbative approximation to the CCSD (Coupled Cluster Singles-Doubles) method, in which single excitations are included directly in the multi-configurational wave function, as in the CCS (Coupled Cluster Singles) method. Additionally, double excitations, important for taking into account the dynamic correlation, are included approximately, in a perturbative way, similarly as in the Møller-Plesset MP2 second order multi-body perturbation approach. The CC2 method provides high quality of calculations for energies of electronic transitions, as well as molecular geometries and vibrational frequencies, also for molecules in excited states, and the vibronic structure of UV-vis spectra[0-3,5]. In works[H5-H7] I carried out the CC2 calculations using the Turbomole program, with smaller basis sets (aug-cc-pVDZ, cc-pVTZ and aug-cc-pVTZ), while calculations with the largest cc-pVQZ basis were made by Dr Marcin Andrzejak.

In the initial works[H1,H2] quantum-chemical calculations (HF and CIS) were performed using Pople split-valence shell basis sets containing polarization and diffusion functions: 6-31G**, 6-31++G**. In the later works[H3-H7], calculations with DFT and CC2 methods were carried out using a series of Dunning's correlation-consistent basis sets: cc-pVXZ(X=D,T,Q) and aug-cc-pVXZ(X=D,T).

### *Energies of excited electronic states*

The differences in accuracy of quantum chemistry methods are already apparent when excitation energies to the $S_1$ electronic state are compared. The adiabatic transition energies (including ZPE corrections for zero vibrational energies) calculated with DFT(B3LYP) and TDDFT (3.50-3.58 eV) and CC2[H6] (3.49-3.57 eV) methods, is consistent with the experimental value (3.54 eV) with of accuracy not worse than 0.05 eV. The oscillator strength for transition to this state is moderate ($f \approx 0.1$). In contrast, the excitation energy calculated as the difference between the energies of the ground and excited states optimized with HF and CIS methods, respectively, is overshoot by more than half eV and the inclusion of the ZPE correction does not provide any noticeable improvement.

Quantum-chemical calculations have shown that the energies of other excited states of the n→π* and one state π→π* character are more than 1 eV higher[H7] than the energy of $S_1$ state. Moreover, transitions to these states are symmetry forbidden for the σ→π* or n→π* excited states of A'' symmetry, and the transition moment to the next state π→π* (A') is very small ($f \approx 0.035$). In contrast, the π→π*(A') excitation that has large oscillator strength ($f = 0.35$) appears at 5.5-5.8 eV. These results indicate that the investigated $S_1$ state can be inerpreded as the $L_a$ state in Platt notation, and the second π→π* state, with a small transition moment ($f \approx 0.035$) is the state $L_b$, whereas the third excited π→π* state, with a high oscillator force $f = 0.35$ is the $B_b$ state. Therefore, the two absorption bands of anthranilic acid in the UV range in a non-polar solvent (cyclohexane)[20], the first with a moderate absorbance, at $\lambda_{1,\max}$ = 333 nm (3.7 eV), and the strong one, $\lambda_{2,\max}$ = 247 nm (5.0 eV), should be interpreted as the $S_0 \rightarrow L_a$ and $S_0 \rightarrow B_b$ transitions, respectively. On the other hand, the weak transition $S_0 \rightarrow L_b$ and several symmetry forbidden transitions to states A'' related to excitations or n→π* or σ→π* are probably obscured. The above indicates that the possible influence of the vibronic coupling on the vibrational structure of the band $S_0 \rightarrow S_1$ is not discernible due to the large energetic separation of the $S_1$ state from other excited states of appropriate symmetry and large transition moment.

### *The ground-state geometry*

The ground-state equilibrium geometries calculated with DFT(B3LYP) and CC2 methods with tripple-ζ basis sets are very similar to each other[H6], except for noticeable differences in hydrogen bond parameters and C=O bond in the carboxyl group. In contrast, equilibrium geometry calculated by the Hartree-Fock method[H1,H3] differs significantly from the results of other methods. Significant differences  concerns the hydrogen bond parameters and typically moderate differences in bond alternation in the π-electron system of the molecule, not exceeding 1 pm. The ground-state geometry of the molecule calculated using the CC2/aug-cc-pVTZ method, is shown in Fig. 9.

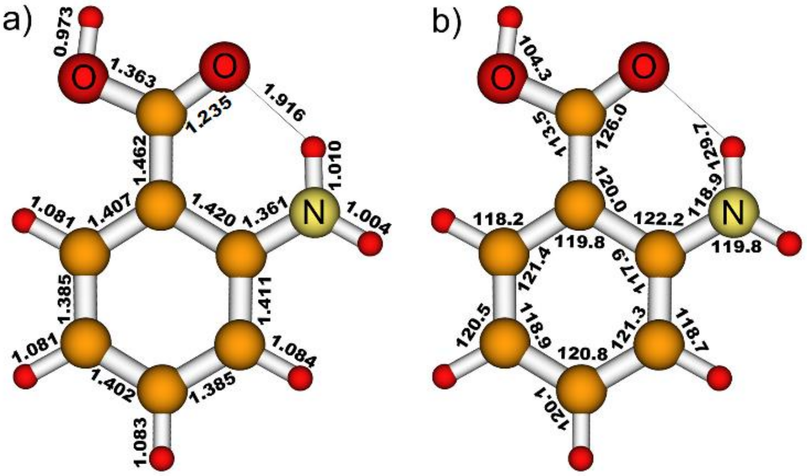

**Fig.9.** [H6] Equilibrium geometry of anthranilic acid molecule in the ground state computed with the CC2/aug-cc-pVTZ: a) bond lengths, b) valence angles.

CC2 and DFT methods predict the presence of a weak O···H hydrogen bond, of length approximately 1.91Å (CC2)[H6], 1.93Å (DFT)[H6] in length, which induces slight asymmetry of the amino group. The angle C–N–H with a free hydrogen atom is about 1° larger than the analogous angle, measured to the hydrogen atom participating in the hydrogen bond, and the length of the N–H bond participating in the hydrogen bonding is about 0.5 pm longer in both methods, than the free N–H bond. In contrast, according to the HF method, the influence of the hydrogen bond in the ground state is practically unnoticeable[H1,H3], the distance O···H, equal to 2.00 Å is about 9 pm greater than in the CC2 method and the asymmetry of the amino group is not discernible.

Bond alternation in the π-electronic system indicates the coupling of substituents with the aromatic ring of the molecule. This hyperconjugation causes also that the $C_2$–COOH bond of the length about 1.46 Å is shorter than a typical single C–C bond by ca. 8 pm. In the aromatic ring, on the other hand, the $C_1$–$C_2$ (1.42 Å)[H6] bond between the carbon atoms at which the substituents are located is weakened. The coupling of an amino group with the aromatic ring is indicated by the $C_1$–N bond length (1.36 Å), shorter than in aniline by about 3 pm and by very low inversion barrier for the $NH_2$ group, and hence, its dynamically planar geometry[37] (Section II.4.3) .

The CC2 and DFT methods[H6] give consistent predictions for the bond lengths in π-electronic system as well as their alternation, and differences between bond lengths usually do not exceed 0.5 pm. Discernible discrepancies appear only for the C=O bond (about 1.23 Å in CC2, 1.21 Å in DFT and 1.20 Å in HF). It is associated with coupling of the COOH group with an aromatic ring, and with a discernible weakening of the C=O bond due to the formation of a weak hydrogen bond, which is slightly weaker in DFT than in CC2. The HF[H1,H3] method, however, predicts the π-electron coupling of substituents with the ring noticeably weaker than in CC2 and DFT. The $C_2$–COOH bond (1.47 Å) is longer by about 1 pm than in those methods, while the following bonds in the aromatic ring: $C_1$–$C_2$ (1.41 Å) bond, and $C_3$–$C_4$ bond and $C_5$–$C_6$ (1.37 Å) are shorter by about 1 pm.

### *Molecular geometry and dynamics in the excited state*

In the excited state S1, the hydrogen bond is much stronger than in the ground state. According to the results of CC2 calculations, its length, R (O···H) is 1.64Å[H6], which indicates the presence of a strong hydrogen bond. However, according to the TDDFT calculation results, its length is 1.74Å[H6]. The geometry of the molecule in the excited state, calculated with the CC2/aug-cc-pVTZ method, is shown in Fig. 10. Considering the level of sophistication and accuracy of the ab initio method used, calculations using the CC2[31,32] coupled cluster method with cc-pVQZ or aug-cc-pVTZ basis sets should be considered the most reliable. Moreover, the higher reliability of these results, with respect to the geometry of the excited state, is confirmed by calculations of FC factors and modeling of band intensities[H7] (Section II.4.5).

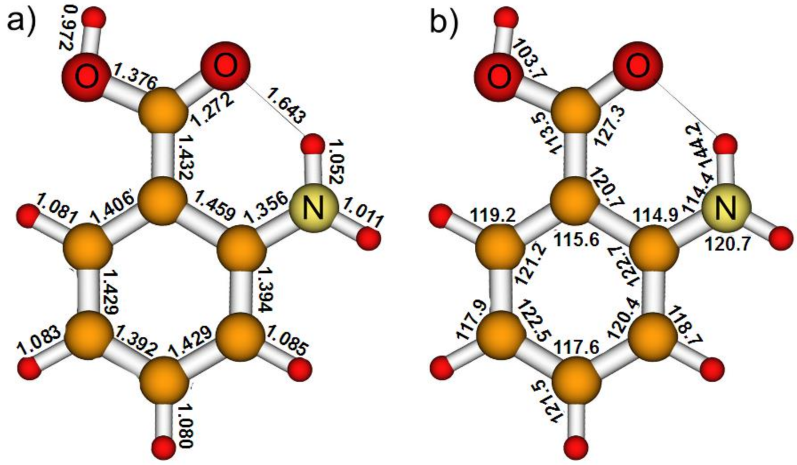

**Fig.10.** [H6] Equilibrium geometry of anthranilic acid molecule in the excited state computed with the CC2/aug-cc-pVTZ: a) bond lengths, b) valence angles.

The quite strong hydrogen bonding causes significant asymmetry of the amine group in which the C–N–H angle with the free hydrogen atom is more than 6° larger (in both methods) than the corresponding angle with the hydrogen atom involved in the hydrogen bond. Moreover, the N–H bond participating in the hydrogen bond is significantly longer, by about 4 pm (CC2) or 3 pm (TDDFT) than the free N–H bond. Whereas the difference of both angles C-C-(COOH), which in the ground state was negligibly small, in the excited state is equal to 3.1°(CC2). In contrast, CIS method foresees the occurrence of quite weak hydrogen bond[H1,H3]; the distance O···H is 1.85 Å and the asymmetry of angles C–N–H is only 3° and the asymmetry of bonds N-H is only 1 pm.

A significant strengthening of the hydrogen bond, which also causes the weakening of the N–H bond that participates in it, is confirmed by the decrease in the frequency of the ν(N–H) stretching vibration. In the ground state, the frequencies of the coupled N–H stretching vibrations (3394 cm$^{-1}$ and 3542 cm$^{-1}$)[22] are separated by about 150 cm$^{-1}$, which is a typical split value between a symmetric and antisymmetric combination of stretching vibrations of individual N–H bonds amino group. Quantum-chemical calculations with all methods used for this state (HF[H1,H3], DFT[H3,H6], MP2[38], CC2[H6]) well reflect the magnitude of this splitting. In the excited state however, the N–H stretching vibrations are uncoupled and localized due to the involvement of one of the hydrogen atom in the hydrogen bond with the carboxyl group. This was confirmed by analyzes of the Dushinsky matrix[H3] and the 98% contribution of the localized vibrations in the potential energy distribution distribution[H4] PED. The N–H stretching vibrations involving the free hydrogen atom has a frequency of 3460 cm$^{-1}$, which is typical for ν(N–H) and is also close to the average of the $\nu_{sym}$(N–H) and the $\nu_{asym}$(N–H) vibrational frequencies in ground state. In contrast to the above, the experimentally determined frequency (the IR-UV double resonance spectra[22]) of stretching vibrations of the N–H bond involving the H-bonded hydrogen atom is dramatically reduced, up to 2900 cm$^{-1}$, which indicates a significant weakening of this bond. Due to the significant discrepancies between the experimental and theoretical frequencies calculated with various methods, and differences in the scaling factor[39], especially for the high-frequency oscillations, a more appropriate measure of the weakening of the discussed bond than the is the difference between the frequencies of both N–H vibrations of experimental value 560 cm$^{-1}$. The CIS method predicts a drastically underestimated value of this difference[H3] of only 255 cm$^{-1}$, i.e. only about 100 cm$^{-1}$ larger than a typical value of the splitting between symmetrical and anti-symmetrical combination of N–H stretching vibrations in the amine group. The results of the vibrational analysis performed with TDDFT[H3,H6] and CC2[H6] methods reflect this frequency difference much better (TDDFT: 460-500 cm$^{-1}$, CC2: 715-760 cm$^{-1}$). These results suggest however, that the TDDFT method slightly underestimates this effect and the CC2 method noticeably overestimates it.

In the $S_1$ excited state the π-electronic coupling of substituents with the aromatic ring is much stronger than in the ground state. This is mainly indicated by the significant shortening of the C–COOH bond, of the length 1.43Å (CC2[H6]) and 1.45Å (TDDFT[H6]), which is almost the same as the the length of the $C_3$–$C_4$ and $C_5$–$C_6$ bonds in the aromatic ring in this state. In contrast, the $C_1$–$C_2$ bond is significantly weakened and unusually extended as for aromatic bond in the benzene ring and reaches the length of 1.46 Å (CC2) and 1.45 Å (TDDFT). What is more, the results of CIS calculations predict excessive weakening of this $C_1$–$C_2$ bond and is lengthening up to 1.48 Å. Lengths of other bonds in the ring are almost equal to each other according to the CIS results, with values of 1.40-1.41 Å. The significant bonds alternation in the π-electron system indicates a strong hyperconjugation, which can be interpreted as a significant contribution of the resonance structure, in which a double bond connects carboxyl group and the ring, while the $C_1$–$C_2$ bond in the aromatic ring becomes a single bond. In addition the $C_3$–$C_4$ and $C_5$–$C_6$ bonds are also noticeably weakened. Significant changes concern the weakening and elongation of the C=O bond, which is partly due to the coupling of the COOH group with an aromatic ring, and partly to the formation of a strong hydrogen bond between the oxygen atom and the amino group. Since these phenomena are taken into account to most accurately by the CC2 method, the most reliable value is the bond length C=O is 1.27 Å, less reliable is the TDDFT value 1.25 Å and the CIS estimation 1.22Å is the least reliable.

### ***Basis set dependence of the computed geometry parameters***

In order to monitor the dependence of the calculated geometry parameters on the basis sets used and to approach the complete basis set limit (CBS), the DFT and CC2 calculations were performed using a series of correlation consistent Dunning basis sets: cc-pVXZ(X=D, T,Q) and aug-cc-pVXZ(X=D,T). The deviation from the complete basis set limit for the length of valence bonds is close to 0.1 pm when calculated using these basis sets, which is sufficient a the practical point of view. This is justified because it has been proved in the literature that for the closed-shell molecules, deviations of the calculated bond lengths from the CBS limit smaller than 0.1 pm are obtained using the MP2 method with the aug-cc-pVTZ basis set, and using the CCSD(T) method with cc-pVQZ[40]. Good convergence of DFT(B3LYP) calculations is usually obtained more easily than for MP2.

The dependence of the most important geometry parameters on the basis sets can be monitored on the example of the length of the O···H hydrogen bond (Fig. 11) and the complete lists of the geometry parameters are presented in work[H6]. The change in the length of hydrogen bond is so symptomatic because it is the biggest difference in the equilibrium geometry between the investigated $S_0$ and $S_1$ states, and it is very sensitive not only to the choice of quantum chemistry methods, but also to the basis sets. Moreover, the shortening of the hydrogen bond imposes significant changes of valence angles (Fig. 12) within substituents and the angles located at the $C_1$ and $C_2$ carbon atoms in the aromatic ring.

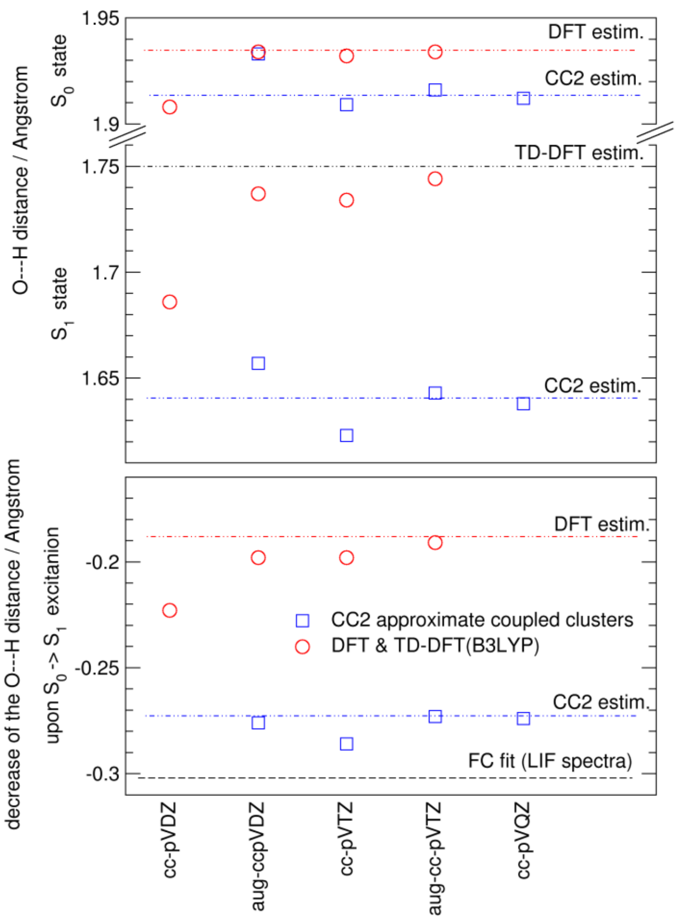

**Fig.11.** [H6] The basis set dependence of the H···O distance (top plot) and the change of the equilibrium length of the hydrogen bond upon the $S_0 \rightarrow S_1$ excitation as computed with the CC2 and TDDFT methods.

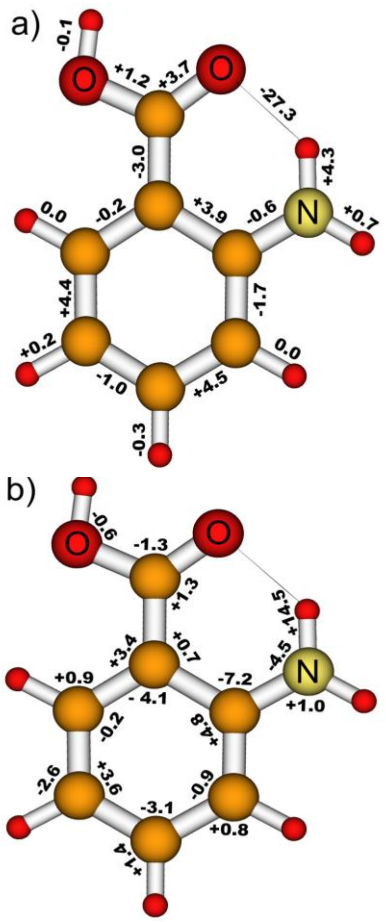

**Fig.12.** [H6] The differences in the equilibrium geometry of anthranilic acid molecule between the $S_0$ and $S_1$ states computed with the CC2/aug-cc-pVTZ: a) differences of bond lengths, b) differences of valence angles.

Within the selected quantum-chemical method, very good agreement of the calculated geometry parameters and their differences upon the excitation is achieved in larger basis sets. In the CC2 method, consistency of results for the ground state is obtained starting from the cc-pVTZ basis, while for the excited state starting from the aug cc-pVTZ basis. In the DFT method, the consistency of results is obtained starting from the cc-pVTZ basis set for both states. The results calculated in the double-$\zeta$ bases show a significant discrepancies. The discrepancies of results for the excited state is significantly larger than for the ground state. However, due to the fact that the direction of these deviations in each basis set from the asymptotic value is usually the same for both electronic states, the discrepancies of the calculated changes in equilibrium geometry are smaller than the discrepancies of the geometry parameters for the excited state. Thus, partial compensation of errors improves the accuracy of these predictions of the changes in equilibrium geometry, which is important for modeling FC factors and band intensities.

### *II.4.5 MODELING OF FRANCK-CONDON FACTORS*

Multidimensional FC factors take into account not only the impact of changes in the equilibrium geometry of the molecule on the intensities of electron-oscillating bands, but also the influence of changes in vibrational frequencies and the Dushinsky effect associated with the so-called "mode mixing". I modeled the intensities[H1,H3,H7] of vibronic bands in the LIF spectra on using recursive equations for calculating multidimensional FC factors in Cartesian coordinates, derived by Doktorov[30], and using effective calculation algorithms developed by Gruner[34] and Ruhoff[35,36] and colleagues. I implemented these algorithms together with colleagues, with Dr. Katarzyna Pirowska, in the form of procedures of Matlab program used in publication [H1], and in later works [H3, H7] in the form of procedures for Scilab program, programmed together with dr Sebastian Leśniewski. In the FC modeling I took into account over 4000 vibrational states of the molecule in the excited electronic state. Among them there are overtones up to $\upsilon = 6$ for the two most important vibrations forming long progression ($253\ \mathrm{cm}^{-1}$ and $418\ \mathrm{cm}^{-1}$) and overtones up to $\upsilon = 4$ for the other in-plane vibrations of frequencies up to $900\ \mathrm{cm}^{-1}$, as well as overtones up to $\upsilon = 2$ for all other in-plane vibrations.

Comparison of the spectra modeled on the basis of TDDFT and CC2 calculations with the experimental LIF spectrum is shown in Fig.13. It shows that the differences in intensity between the spectra modeled on the basis of the results of calculations with the same quantum-chemical method but in different basis sets are small, of magnitude only a few percentage points at most. On the other hand, significant differences occur between the spectra modeled on the basis of the results of calculations with different quantum-chemical methods, and between the modeled spectra and the experimental one. In all spectra, two vibrations ($253\ \mathrm{cm}^{-1}$ and $418\ \mathrm{cm}^{-1}$) generate very strong bands and form two main progressions. In addition, there are combinations of these vibrations with other totally-symmetric vibrations which, together with the dominant progressions, generate a rich vibronic structure of the investigated electronic band, containing more than a hundred vibronic bands of moderate or low intensity. Noticeable congestion of vibronic bands begins in the spectral range starting from about $500\ \mathrm{cm}^{-1}$ above the adiabatic transition, and significant congestion of vibronic bands appears in the range above $1000\ \mathrm{cm}^{-1}$.

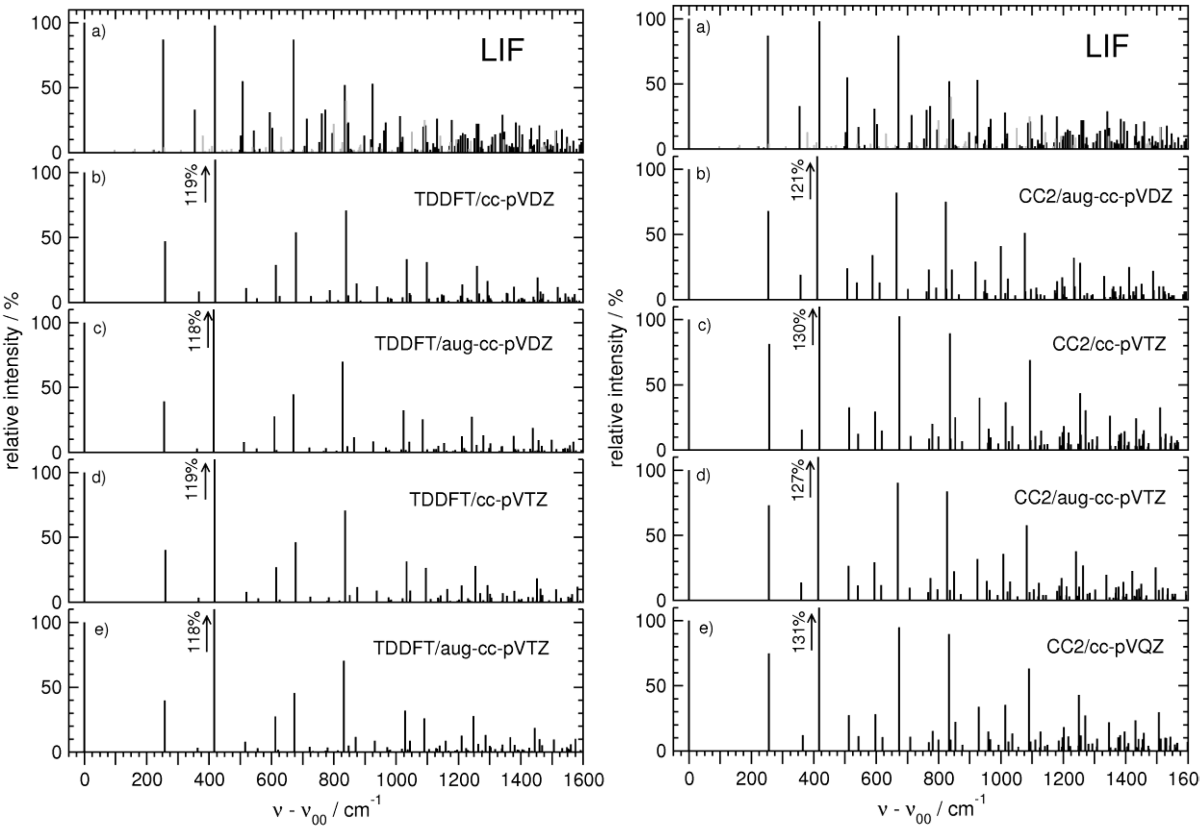

**Fig. 13.** [H7] The spectra modeled within the MFC model using the TDDFT or CC2 results compared with the LIF spectrum (LIF bands assigned to out of plane modes or unassigned are printed in gray).

**Fig. 14.** [H3] The spectra modeled within the 1-D F and MFC model using the CIS or TDDFT results compared with the LIF spectrum (LIF bands assigned to out of plane modes or unassigned are printed in gray).

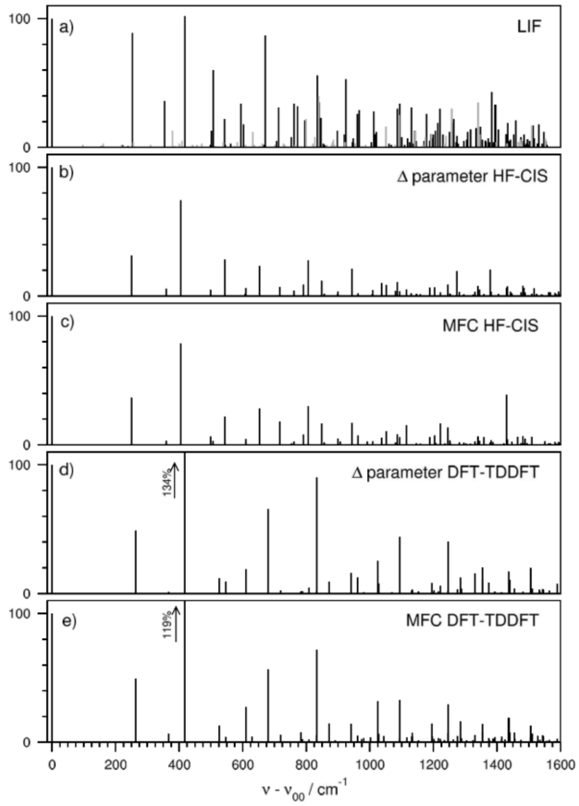

The spectra modeled on the basis of TDDFT calculations contrast more clearly with the experimental spectrum than those obtained from CC2 calculations. Compared to the experimental values, the intensities of fundamental transitions are significantly lower in the TDDFT spectra, which results in even more pronounced loss of intensity of their overtones, with an increase in the vibrational quantum number (with the exception of overestimated intensities for the bands associated with the 418 cm$^{-1}$ vibration). Spectra obtained from CC2 calculations show much better agreement with the experimental spectrum, both in terms of the overall intensity distribution in the spectrum and the intensities of individual bands. The worst agreement with the experimental spectrum, due to a drastic underestimation of band intensities, is shown by the spectra modeled on the basis of CIS method for the excited state and Hartree-Focka[H2,H3] method for the ground state, whose comparison with TDDFT spectra is shown in Fig. 14. Such a drastic underestimation of intensity in HF-CIS spectra results from a drastic underestimation of equilibrium geometry changes upon the excitation, determined by these methods[H1,H3]. This in turn results from improper modeling of properties of hydrogen bonds, related to the lack of the electronic correlation in both these methods, which are limited to the averaged field model of all interacting electrons.

In order to emphasize the influence of other factors, in addition to displacement parameters, on the calculated FC factors and on the fitted geometry changes, calculations were also performed in a one-dimensional model of displaced harmonic oscillators DHO. Comparison of the spectra obtained with both models (shown in Fig. 14) shows that taking into account, in addition to displacement parameters, the influence of the omitted factors causes only negligible discrepancies of modeled spectra. Additionally, using the one-dimensional model, the intensities for overtones and combination transitions in the experimental spectra[H2,H4,H5] was also modeled on the basis of intensities of the fundamental transitions (Section II.4.1). These analyzes and comparisons showed that in the investigated spectra the Dushinsky effect plays a negligible role, and the differences between the results obtained in both models of FC factors (one- and multi-dimensional) are insignificant[H3,H7]. In addition, performing calculations in a one-dimensional model facilitated the analysis of the mutual impact of observed band intensities and geometry changes[H7].

The Dushinsky effect stems from the differences between the normal vibrations of the molecule in both electronic states, and their change upon the electronic excitation is called of mixing of normal vibrations or "mode mixing". The quantitative measure of the mode mixing upon the excitation is the Dusinski's matrix, representing the transformation between the normal vibration vectors of a molecule in both states. The elements of this matrix are equal to the projections of normal mode vectors of a molecule in one electronic state on the vibration vectors of the other state. Because these vectors, expressed in mass-weighted coordinates are normalized and orthogonal, Dushinsky matrix is orthogonal, and squares of its elements sum up to one in rows and columns of this matrix. Thus the squares of the elements of Dushinsky matrix are provide a strict quantitative measure of the mode mixing and the similarity of the molecular vibrations in both electronic states. Similarly, the matrix of transformation between normal coordinates calculated by various quantum chemistry methods for a molecule in the same electronic state is also orthogonal. In Fig. 15, the Dushinsky matrix calculated using the Hartree-Fock and CIS methods and with the FDT and TD-DFT methods, as well as the transformation matrices between normal modes calculated for the ground state with the Hartree-Fock and DFT methods and for the excited state with the CIS and TDDFT methods are presented in graphical form. In the matrices shown in Fig. 15, the rows and columns numbered from 1 to 31 indicate totally-symmetric vibrations, while the remaining 14 indicate out-of-plane vibrations.

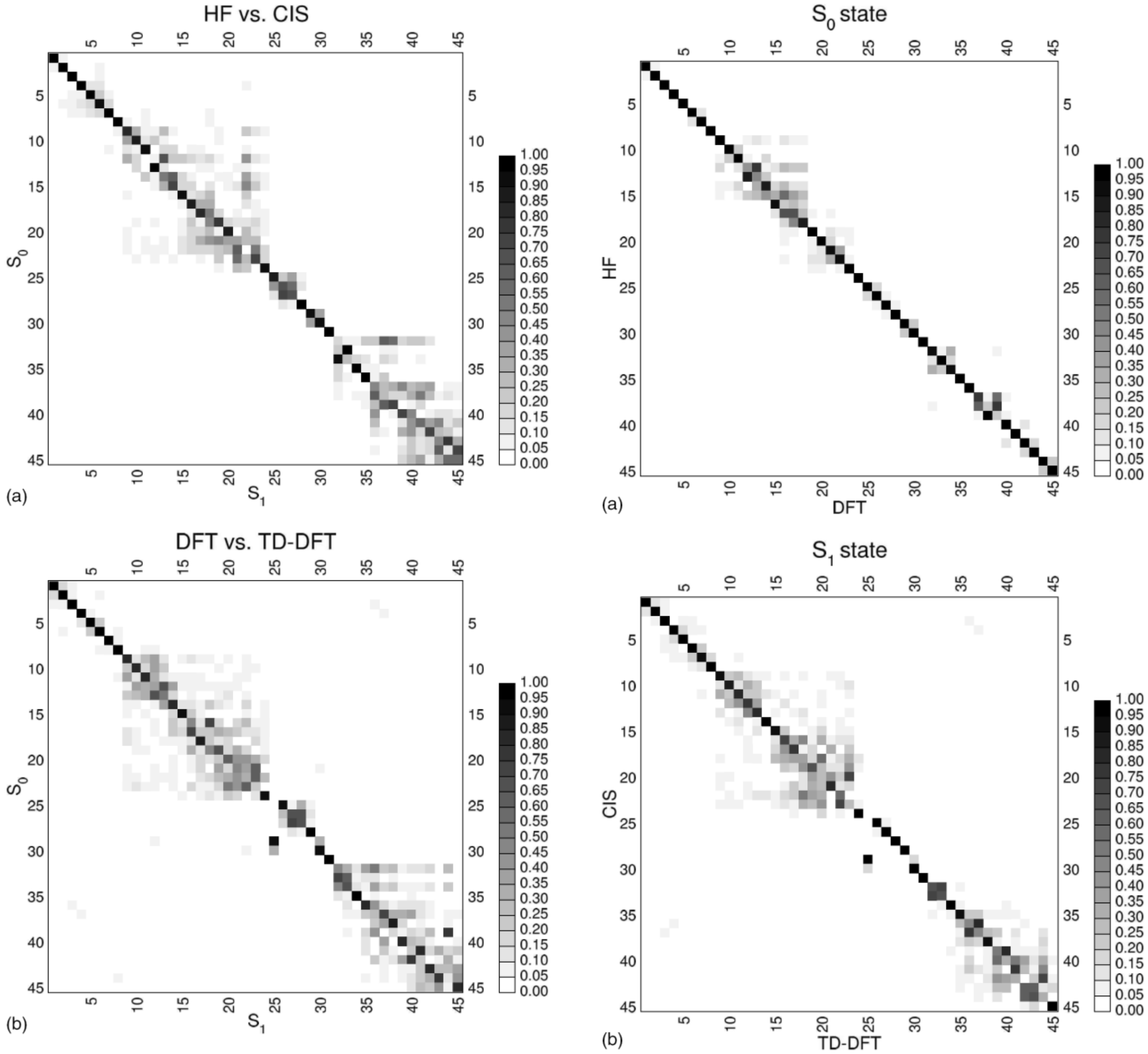

**Fig. 15.** [H3] Maps of absolute values of the Dushinsky matrix elements (left) and the matrices of normal mode transformations: for the ground state calculated with the Hartree-Fock and DFT(B3LYP) methods, and for the excited state calculated with the CIS and TD-DFT(B3LYP) methods.

Strong mode mixing upon the electronic excitation is predicted by both groups of methods in almost separated blocks of totally-symmetric vibrations: a) in the range of medium frequencies (vibrations of the numbers 9-24 and frequencies in the range 1000-2000 cm$^{-1}$); b) in the block of C–H stretching vibrations; and c) in the two-dimensional the block of N–H stretching vibrations. In addition, the strong mode mixing is predicted for almost all off-plane vibrations. Some vibrations project on two or three vibrations of the other electronic state with almost equal contributions (squares of projection coefficients), for these vibrations it is impossible to identify unambiguously their equivalents in the second state. However, almost all high-intensity bands are associated with in-plane vibrations of frequencies below 1000 cm$^{-1}$, or are their overtones or combinations. They are hardly affected by the Duszyński effect, which was confirmed both on the basis of the results of quantum-chemical calculations, as well as by analyzing the intensities in experimental spectra[H2,H4,H5] (Section II.4.1). In addition, their identification is unquestionable and further confirmed by the study of isotopic effects[H4,H5] (except for the 7S vibration). Therefore, the intensities of low-frequency fundamental transitions carry most of the information about changes in the molecular geometry, hardly perturbed by the Dushinsky effect.

From the formal point of view, the transformation of normal modes calculated with various quantum-chemical methods is analogous to the transformation described by Dushinsky matrix. The calculated vibrational modes result from simultaneous diagonalization of the Hessian matrix and the matrix of the kinetic energy operator. Vibrational modes computed with various quantum chemistry methods differ from each other and the matrices of these transformations differ identity matrices because the Hessian matrices are different while the matrix of the kinetic energy operator remain unchanged. Differences concerning the Hessian matrices of two different electronic states describe the real physical phenomenon, related to changes of force constants for bonds and angles upon the electronic excitation. Whereas a significant physical difference between these cases consists in the fact, that different Hessians calculated for a molecule in the same electron state using two quantum-chemical methods, result from differences concerning theoretical description of the same physical state of the molecule. However, in both cases the transformation matrices are orthogonal and provide a quantitative measure of the similarity of the normal vibration vectors whose transformation they describe. Therefore, it can be concluded that the transformation of normal modes calculated with different quantum-chemical methods describes in a way the effect of mixing of normal vibrations between quantum-chemical methods.

Transformation matrices between vibration vectors calculated by different quantum-chemical methods assume a similar block-diagonal form to that of Duszynski matrix. Quite a good agreement between the calculated normal modes occurs between the results obtained for the ground state molecule with HF and DFT(B3LYP) methods. On the other hand, significant differences occur between the vibrations calculated with CIS method and other methods in the excited electronic state. The differences occur in almost separated blocks of totally-symmetric vibrations: in the medium frequency range, in the block of C–H stretchings; and in the two-dimensional block of the N–H stretchings. Additionally, the strong mixing of vibrations covers virtually all out-of-plane vibrations. Significant discrepancies between the CIS and TD-DFT vibrational modes could make it difficult to identify unambiguously the active vibrations in the spectrum in the mean frequency range. Fortunately, oscillations calculated by DFT or TDDFT and CC2 methods show significantly better consistency for the same electronic state of the molecule and allow for unambiguous identification of active vibrations in the LIF spectrum. In addition, almost all high intensity bands occur in the range below 1000 cm$^{-1}$ or are their overtones or combinations. They are hardly affected by the Dushinsky effect, which has been confirmed both by the results of quantum chemistry[H3,H7] calculations and by the analysis of experimental data[H2] (Section II.4.1). Moreover, their identification is confirmed by isotopic shifts studies.

### *II.4.6 MODELING OF THE CHANGES IN THE EQUILIBRIUM MOLECULAR GEOMETRY ON THE BASIS OF THE EXPERIMENTAL BAND INTENSITIES IN THE LIF SPECTRA*

#### *Fitting of Franck-Condon parameters to the experimental intensities of vibronic bands*

Since my findings proved that the underestimation of modeled band intensities results from too small values of the geometry changes calculated by quantum chemistry methods, I carried out adjustments of the displacement parameters in normal coordinates, to obtain optimal consistency with the experimental band intensities[H3,H7]. The process of the modeling of geometry changes by the fitting of the reduced displacement parameters are shown in Fig. 16. I performed the iterative fitting of FC factors using the least squares by optimizing the values of reduced displacement parameters for selected, most important normal vibrations, for which the amount of reliable experimental data made it possible. The algorithms, which I implemented together with Dr Sebastian Leśniewski, in the form of Scilab procedures, were used in publications [H3] and [H7].

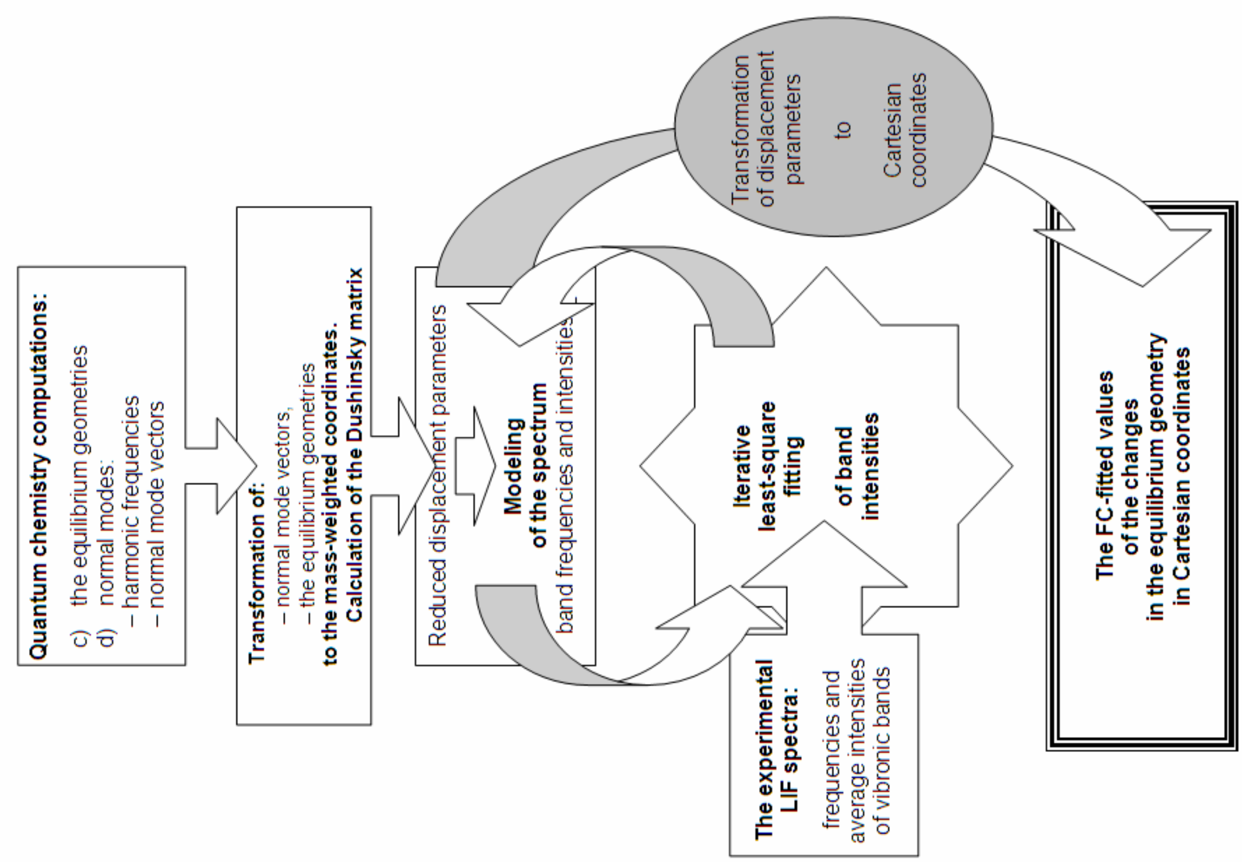

**Fig.16.** Scheme of the modeling of geometry changes by the least square fitting of displacement parameters and FC factors to match the experimental band intensities.

In the final version, the fitting[H7] of the displacement parameters concerned the displacement parameters for 7 totally-symmetric vibrations of frequencies lower than 900cm$^{-1}$. For the remaining 24 plane vibrations, the values of displacement parameters resulting from quantum-chemical calculations were left unchanged for two reasons. Firstly, because even small values of displacement parameters in these 24 normal coordinates may contain important, although dispersed, information about changes in geometry, even though they could not be verified experimentally. Secondly, because they can have an important function in compensation of errors[H7] caused by the use of Cartesian coordinates, instead of curvilinear internal coordinates in the modeling geometry changes based on the fitting FC factor.

Similarly as in the calculations of FC factors, in the modeling of geometry changes I took into account more than 4000 vibrational states of the molecule in the excited electronic state. The displacement parameters were optimized only for those oscillations for which they can be determined from at least a few bands meeting the above criteria. Fig. 17 shows the spectra modeled[H7] on the basis of the selected bands marked with the symbol ○.

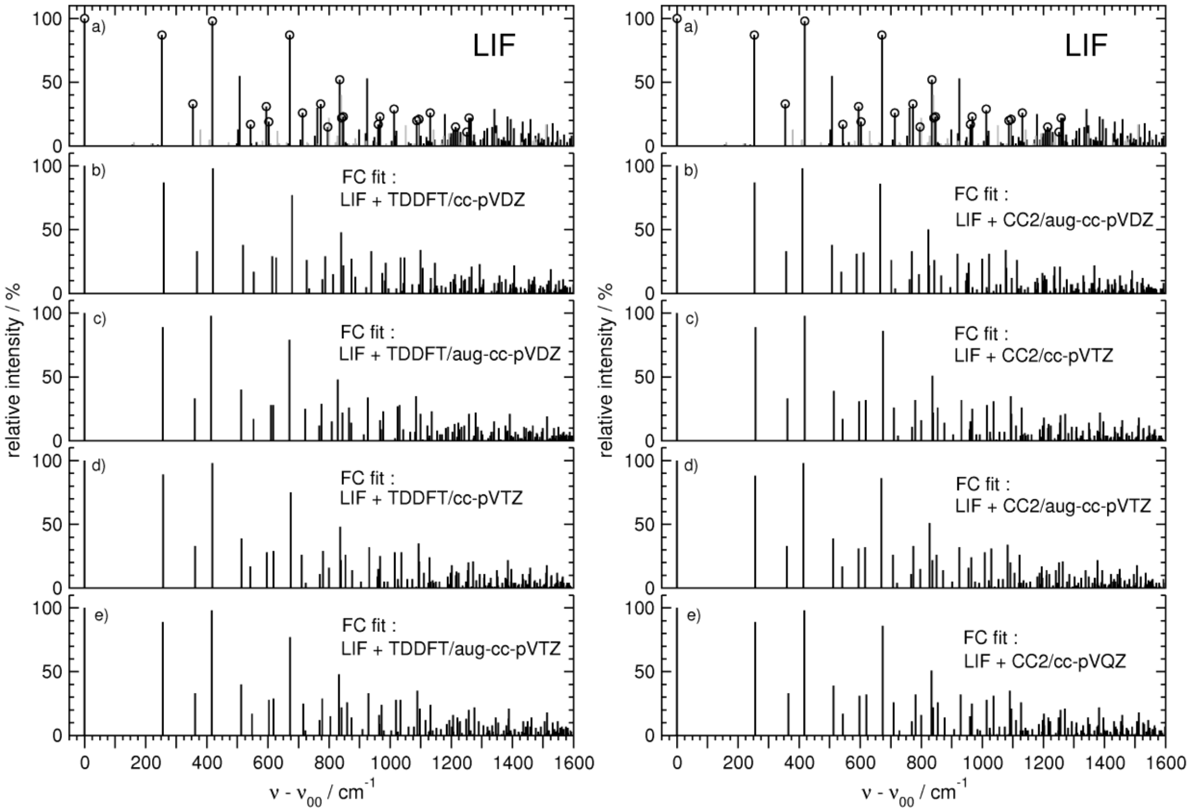

**Fig.17.** [H7] The FC-fitted spectra modeled on the basis of the LIF intensities for the bands marked with circles and the CC2 or TDDFT(B3LYP) normal modes. LIF bands assigned to out-of-plane modes or unassigned are printed in gray.

### *The inverse Franck-Condon modeling: calculation of changes in equilibrium geometry based on experimentally determined displacement parameters*

The components of the vector of geometry changes in the normal coordinates were calculated using the reduced displacement parameters $\Delta_i$ optimized by the fitting of the multi-dimensional Franck-Condon model (MFC). Using the above values the differences of equilibrium geometry in Cartesian coordinates were computed, and finally the changes of bond lengths and valence angles were calculated.

It is easiest to monitor and to quantify the relations between band intensities, displacement parameters and geometry changes in the 1-dimensional model (denoted as Δ-FC model) because in the analyzed case these parameters retain their physical meaning and the dominant impact on the FC factors and band intensities, also in the MFC model. The change of equilibrium geometry induced by electronic excitation in each normal coordinate $Q_i$ is described in the displaced harmonic oscillator model (DHO model) by the reduced displacement parameter $\Delta_i$. Moreover, it is assumed that the coordinates and frequencies of individual oscillations do not change upon the excitation (they do not differ for the molecule in both electronic states). The interpretation based on this model is justified because the deviations from it caused by the influence of the changes in vibrational frequencies and the Dushinsky effect on the band intensities in the studied spectrum are insignificant. This has been demonstrated both by intensity analysis in the experimental spectrum[H2] (Sect. II.4.1) and by calculation of FC factors[H3,H7] based on quantum-chemical calculations (Sect. II..4.5).

In the 1-dimensional model Δ-FC, the relative intensity of vibronic bands $I(\nu_i{}^{\upsilon}_{0})$ (i.e. the intensities of bands divided by the intensity of the adiabatic transition 0-0) for the excitation of the *υ*-th overtones *i*-th normal vibration $\nu_i$, has the simplest form given by the Eq.(8).

$$I(\nu_i{}^{\upsilon}_{0}) = \frac{\Delta_i^{2\upsilon}}{\upsilon!} \tag{8}$$

In this equation $\Delta_i$ is the reduced displacement parameter for the *i*-th normal mode (in the *i*-th normal coordinate) and is equal to the square root of the Huang-Rhys parameter (in the DHO model). The parameters $\Delta_i$ are essential for the magnitude of FC factors and band intensities. They retain their physical meaning also in the MFC model, although their influence on band intensities is entangled in sophisticated recursive equations[33-36], which additionally include diagonal matrices containing vibrational frequencies of the molecule in the ground and excited state and the Dushinsky matrix for this electronic transition. Moreover, the MFC model reduces to the Δ-FC model if the vibrational frequencies remain unchanged in both electron states and the Dushinsky matrix is equal to the identity matrix. The bandwidths for composite combinational transitions are given by the product of the corresponding expressions described in Eq. (8) for the excitations of all normal vibration involved in a given combinational excitation.

The reduced displacement parameter is related to the differences in the equilibrium geometries of both electron states by Eq. (9). The factor $\sqrt{\mu_i\nu_i}$ in this equation can be replaced by $\sqrt[4]{\mu_i k_i}$ , well-known from the quantum harmonic oscillator theory.

$$\varDelta_i = \sqrt{\frac{2\pi^2\nu_i}{hc}}\, D^{\mathrm{MW}}_{\mathrm{ex},\ i} = \sqrt{\frac{2\pi^2\mu_i\nu_i}{hc}}\, D^{\mathrm{Cart}}_{\mathrm{ex},\ i} \tag{9}$$

In this equation, the $D^{\mathrm{Cart}}_{\mathrm{ex},\ i}$ parameter is the *i*-th component of the vector of geometry changes $\vec{D}$ in the normal coordinate $Q_i$ of the molecule in the excited electronic state, expressed by the Cartesian displacements of atoms from their equilibrium positions ($\Delta x_k$ for $k = 1,...,3N$). Whereas the $D^{\mathrm{MW}}_{\mathrm{ex},\ i}$ parameter is a component of the $\vec{D}$ vector in the coordinate $Q_i$ expressed by the displacements of atoms weighted by the square root of the respective atomic masses $\xi_k = x_k\sqrt{m_k}$ and normalized to unity.

Most conveniently, the $D^{\mathrm{MW}}_{\mathrm{ex},\ i}$ parameters can be calculated using the matrix transformation (10), in which $M^{1/2}$ is the $3N\times 3N$ diagonal matrix containing square roots of atomic masses and the columns of $\mathbf{L}^{\mathrm{MW}}$ matrix normal vectors normalized to unity in mass-weighted coordinates.

$$\vec{D}^{\mathrm{MW}}_{\mathrm{ex}} = \mathbf{L}^{\mathrm{MW},\,T}_{\mathrm{ex}}\left(\vec{\boldsymbol{\xi}}^{\mathrm{eq}}_{\mathrm{ex}} - \vec{\boldsymbol{\xi}}^{\mathrm{eq}}_{\mathrm{gr}}\right) = \mathbf{L}^{\mathrm{MW},\,T}_{\mathrm{ex}} M^{1/2}\left(\vec{x}^{\mathrm{eq}}_{\mathrm{ex}} - \vec{x}^{\mathrm{eq}}_{\mathrm{gr}}\right) \tag{10}$$

Transformation of Eq.(10) yields the matrix equation (11).

$$\Delta\vec{x}^{\mathrm{eq}} = \vec{x}^{\mathrm{eq}}_{\mathrm{ex}} - \vec{x}^{\mathrm{eq}}_{\mathrm{gr}} = M^{-1/2}\mathbf{L}^{\mathrm{MW}}_{\mathrm{ex}}\vec{D}^{\mathrm{MW}}_{\mathrm{ex}} \tag{11}$$

In order to calculate changes of the equilibrium geometry in Cartesian coordinates on the basis of the experimental data, the $D^{\mathrm{MW}}_{\mathrm{ex},\ i}$ vector calculated by transformation of Eq (9) is substituted into Eq. (11).

### *Excitation-induced changes in the equilibrium geometry modeled on the basis of experimental band intensities in the LIF spectrum*

The greatest change in equilibrium geometry is the shortening of the intramolecular hydrogen bond. On the basis of my research I have established that the most reliable estimation of the magnitude of this change is the shortening of the distance of the amine hydrogen atom from the carbonyl oxygen atom by $\Delta R(\mathrm{O}\cdots\mathrm{H}) = -31$ pm ±1.5 pm[H7]. This value was established on via least-square fitting of the Franck-Condon factors to the intensity of vibronic bands in the LIF spectrum, using normal vibrations calculated by CC2 method (FC fit: LIF+CC2[H7]). This value was determined in a multidimensional model of Franck-Condon factors (MFC), taking into account the variability of results caused by calculations in a series of basis sets and errors of the experimental intensities. Whereas the fits carried out using DFT and TD-DFT[H3,H7] (FC fit: LIF+DFT) calculations predicted values in the range –(29-32) pm.

<u>Obtaining the above consistency of results is an important achievement of modeling of geometry changes via least-square fitting of FC factors to experimental band intensities in the LIF spectrum with the aid using normal vibrations calculated with two high-quality quantum chemistry methods. It is particularly remarkable when compared to geometry changes calculated using various quantum chemistry methods, which are not only clearly underestimated but also showed very large discrepancies.</u> These ab initio methods predicted the shortening of O···H distance to be within the range from –14.6 pm[H3] with HF and CIS methods, through –22.6 pm[19] in DFT(B3LYP) and TDDFT/cc-pVDZ, and –(19.1-19.8) pm[H6] with the same methods but in aug-cc-pVDZ, cc-pVTZ and aug-cc-pVTZ basis sets, up to –(27.3-28.6) pm[H6] with CC2 method, in aug-cc-pVDZ, cc-pVTZ, aug-cc-pVTZ and cc-pVQZ basis sets.

Comparison of changes in the length of hydrogen bond O···H, calculated by quantum-chemical methods[H6] and the results of the modeling via least-square fitting of Franck-Condon[H7] factors in 1-dimensional and multidimensional model: (FC fit: LIF+CC2, FC fit: LIF+DFT), using a series of basis sets is shown in Fig. 18. The discrepancies of the changes in the O···H distance caused by the use of various basis sets with the same quantum chemistry method have of magnitude 3-4 pm (symbols ○ for TDDFT and ● CC2 in Fig. 18). However, the discrepancies between the results of the fitting of FC factors to the experimental data are moderate, not exceeding 1 pm, and after excluding the results modeled with the cc-pVDZ basis set, are reduced to a few tenths of the picometer.

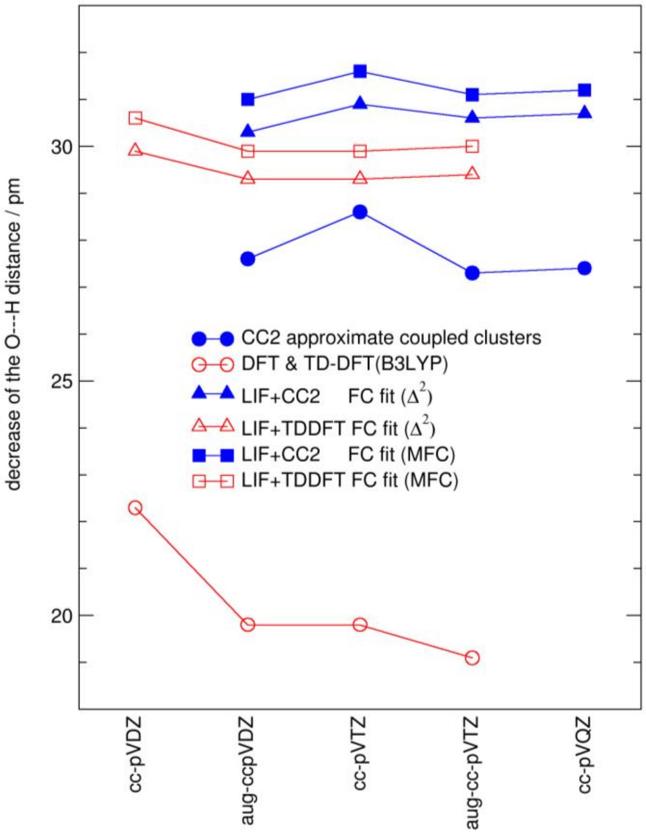

**Fig.18.** Changes in the O···H distance estimated via FC fitting and *ab initio* methods [H7].

The shortening of the hydrogen bond forces the substituents to approach and the deformations of the valence angles, manifested by the presence in the LIF spectrum of the pendulum vibration progression of the substituents, with some contribution of their deformations. The most reliable values of geometry changes are given by FC fit modeling: LIF+CC2[H7]. The results obtained in this model using the aug-cc-pVTZ basis sets are shown in Fig.19, whereas the full list of the geometry parameters included in article[H7] shows that the results of analogous modeling with the cc-pVQZ base differ only slightly from the above.

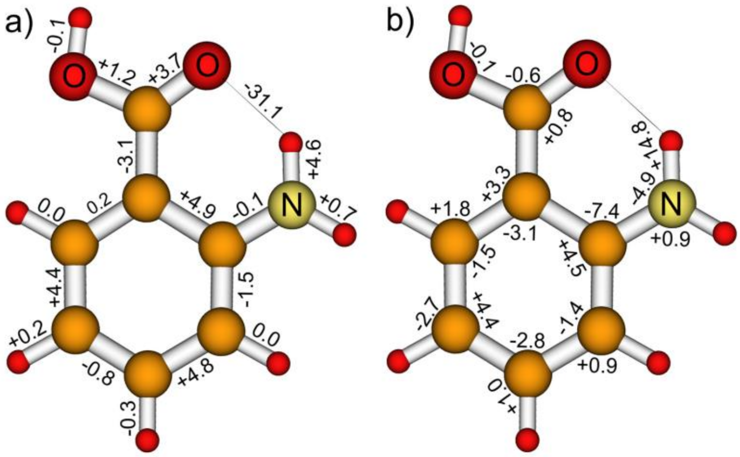

**Fig. 19.** Changes of the equilibrium geometry parameters for anthranilic acid upon the $S_0 \rightarrow S_1$ excitation obtained using the multidimensional FC fitting procedure (MFC) with the aid of the CC2/aug-cc-pVTZ vibrational analysis: a) bond lengths /pm, b) valence angles in degrees[H7].

The geometry changes evaluated using the FC fit: LIF+TDDFT[H7] shown in Fig.20 are similar to the results of FC fit: LIF+CC2, although they are generally noticeably smaller. Differences between these models do not exceed 1 pm for changes of bond lengths and 1° for valence angles. It is worth noting that the discrepancies between the results of modeling of FC fit: LIF+CC2H7 and FC fit: LIF+TDDFTH[H7] are significantly smaller than the discrepancies between the geometry changes computed solely via geometry optimization with these quantum chemistry methods, which approach 2 pm for the changes in the length of valence bonds and 2° for the changes of valence angles[H6].

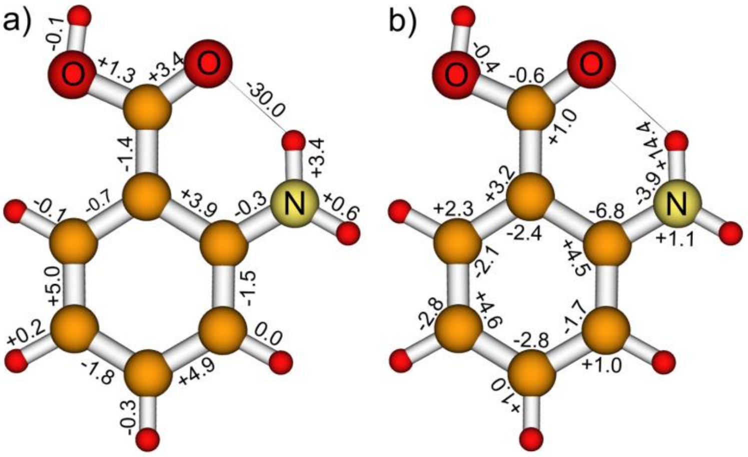

**Fig. 20.** Changes of the geometry parameters for anthranilic acid upon the $S_0 \rightarrow S_1$ excitation obtained using the MFC model fitting procedure with the aid of the TDDFT(B3LYP)/aug-cc-pVTZ vibrational analysis: a) bond lengths /pm, b) valence angles in degrees.

According to the results of FC fit modeling: LIF+CC2[H7], the largest deformation is the decrease of $C_2$–$C_1$–N angle by about 7.5°. The remaining deformations of magnitude 3°–5° concern the valence angles within the aromatic ring[H3,H7], the $C_1$–N–H angle involving the hydrogen atom that participates in the hydrogen bonding as well as the angle $C_3$–$C_2$–(COOH). The electronic excitation induces also lengthening of the N–H bond participating in the hydrogen bonding and changes in bond alteration within the π-electronic system of the molecule. The changes in the bond alternation concern mainly the lengthening of bonds $C_1$–$C_2$, $C_3$–$C_4$ and $C_5$–$C_6$ in the aromatic ring of magnitude up to 5 pm, and the C=O bond in the carboxylic group by almost 4 pm. In contrast, the C–C bond that connects the carboxylic group with the aromatic ring is significantly shortened by about 3 pm, indicating significant strengthening of π-electron coupling of the carboxylic group with the aromatic ring.

Geometric considerations lead to the conclusion that the shortening of the hydrogen bond is mainly possible due to the deformation of valence angles, leading to the displacements of substitutes towards each other. First of all, the reduction of the $C_2$–$C_1$–N angle gives the contribution about 40-50% to the shortening the O···H distance and almost the entire contribution to bringing oxygen and nitrogen atoms closer. A further 35-40% of the reduction in the O···H distance should be attributed to the decrease of the $C_1$−N−H angle.

### *The excited-state molecular geometry modeled on the basis of experimental intensities*

Geometry changes determined by the fitting of FC factors to the bands intensities in the LIF spectra can also be used to determine the geometry parameters of the molecule in the excited state, since the ground-state geometry is already evaluated with good accuracy, both from experimental studies and from calculations using various quantum chemistry methods, for which the consistency between the results obtained using different methods is significantly better than for the excited state

Regarding the level of sophistication and accuracy of the ab initio method used, the calculation of the CC2 coupled cluster method should be considered as the most reliable one, moreover, the better agreement of its results with respect to the geometry of the excited state is also confirmed by the results of the FC modeling of the band intensity (Sect. II.4.5)in the LIF spectrum[H7]. The geometry shown in Fig. 21 should be considered the most accurate estimation of the geometry of the molecule in the $S_1$ excited state. It was determined on the basis of modeling of geometry changes by least-square fitting of FC factors to the intensities in the LIF spectra, in the multidimensional model, with the aid of normal vibrations calculated using CC2 method (FC fit: LIF+CC2/cc-pVQZ)[H7], and on the basis of the ground-state molecular geometry calculated using CC2/cc-pVQZ[H6]. Such a choice is justified because it has been proved in the literature that for closed-shell molecules, the discrepancies from the complete basis set limit (CBS limit) smaller than 0.1 pm for the calculated bond lengths, are obtained with the MP2 method in the aug-cc-pVTZ basis set and with the CCSD(T) method in the cc-pVQZ[40] basis. It is considered that the CC2 method gives better accuracy than MP2, and comparable or in some aspects better than CCSD[31,32]. Therefore it should be assumed, that its requirements for the quality and size of basis sets, are similar to the above mentioned ones. Furthermore, the results of the CC2/aug-cc-pVTZ and CC2/cc-pVQZ[H6] calculations are consistent with each other, as well as the results of the modeling of geometry changes by fitting of FC factors to the LIF spectra carried out on the basis of the normal vibrations calculated by these methods[H7].

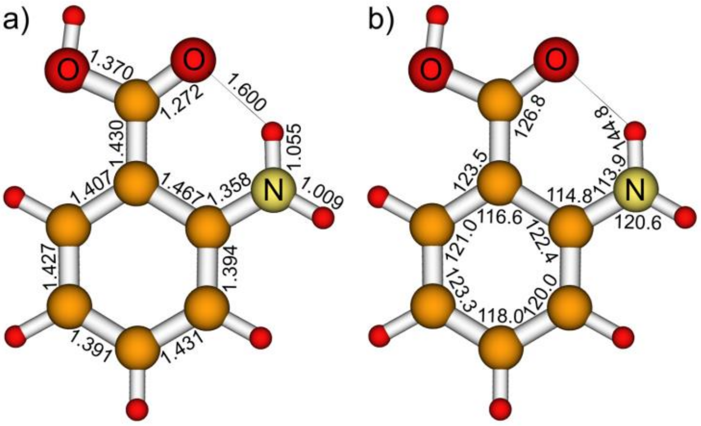

**Fig. 21.** The equilibrium geometry of the anthranilic acid molecule in the $S_1$ excited state, determined as the sum of the ground state geometry calculated with the CC2/cpVQZ[H6] method and the geometry changes upon the excitation determined by FC fit:LIF+CC2[H7]: (a) bond lengths[Å], (b) valence angles.

In the $S_1$ excited state, the hydrogen bond is much stronger than in the ground state[H6]. According to the results of FC-fit: LIF+CC2 the O···H distance is reduced to 1.60±0.015 Å[H7]. This indicates the presence of quite strong hydrogen bond, especially when significant rigidity of the molecular skeleton is considered, which makes obtaining of closer proximity of COOH and $NH_2$ groups quite difficult. The O···H distance is much shorter than in the ground state ($S_0$:

1.91 Å, CC2). Moreover, the value 1.60 Å ($S_1$, CC2+FC fit) determined on the basis of experimental results is noticeably smaller than the value calculated by geometry optimization for the excited state with the CC2 method (1.64 Å)$^{H6}$.

The strong hydrogen bonding causes significant asymmetry of the amino group in which the C–N–H angle with the free hydrogen atom is more than 6.7° larger than the corresponding angle involving the hydrogen bonded H atom and the difference between both C–C–N angles reaches 8°. Moreover, the length of the N–H bond participating in the hydrogen bond is significantly larger, by about 4.5 pm than the free N–H bond. The difference of both angles C–C–(COOH) characterizing the position of the carboxylic group with respect to the aromatic ring, which in the ground state was negligibly small, approaches 3.6° in the excited state.

The evaluated bond alteration in the $\pi$-electronic system is comparable to results calculated with the CC2 method. In the $S_1$ excited state the $\pi$-electronic coupling of karboxylic group with the aromatic ring is much stronger than in the ground state. This is indicated mainly by significant shortening and strengthening of the C–COOH bond, whose length 1.43 Å (the same as computed with CC2$^{H6}$) is actually equal to the length of the $C_3$–$C_4$ and $C_5$–$C_6$ bonds in the aromatic ring in the excited state. The $C_1$–$C_2$ bond of the length 1.47 Å is the longest bond in the aromatic ring (according to FC fit: LIF+CC2). Such a significant bond alteration in the $\pi$-electron system indicates a strong hyperconjugation. This can be interpreted in terms of significant contribution of the resonance structure, in which is a double bond is formed between the carboxylic group and the ring, while the $C_1$–$C_2$ bond in the aromatic ring is a single bond. In addition, the $C_3$–$C_4$ and $C_5$–$C_6$ bonds are noticeably weaker than in the ground state. Significant changes concern also weakening and lengthening of the C=O bond to 1.27 Å, which is related partly to the coupling of COOH group with the aromatic ring and partly to the creation of strong hydrogen bond between the oxygen atom and the amino group.

### *II.4.7 ANALYSIS OF THE COMPLETENESS AND ACCURACY OF THE MODELING*

#### ***Contribution of individual oscillations and completeness of the modeling of geometry changes***

In order to estimate the contribution of geometry changes in individual normal coordinates to the total changes in the equilibrium geometry I analyzed the relations between the reduced displacement parameters $\Delta_i$ and the displacements of atoms in normal modes expressed in Cartesian coordinates $D_i^{\mathrm{Cart}}$ or in mass-weighted coordinates $D_i^{\mathrm{MW}}$ as well as the intensities of fundamental transitions, within the 1-dimensional model of FC factors (DHO). This approach is sufficient because the influence of other factors, not taken into account in this model on band intensities is negligible in the studied spectrum. Transformation of Eq. (8) and Eq. (9) leads to quadratic dependence for intensities of fundamental transitions (for $\upsilon = 0 \rightarrow 1$) on displacement parameters $\Delta_i$, given by Eq. (12).

$$I(\nu_{i\,0}^{\;1}) = \Delta_i^2 = \frac{2\pi^2}{hc}\nu_i D_{\mathrm{ex},\,i}^{\mathrm{MW}\,2} = \frac{2\pi^2}{hc}\mu_i \nu_i D_{\mathrm{ex},\,i}^{\mathrm{Cart}\,2} \tag{12}$$

The factor $\mu_i\nu_i$ increases the influence of geometry changes in normal coordinates associated with high-frequency vibrations or vibrations having large reduced mass on the intensities of the corresponding fundamental transitions. The dominant factor is the impact of increasing frequencies, from about 250 cm$^{-1}$ to over than 3500 cm$^{-1}$ (for the in-plane modes of the anthranilic acid molecule). This influence is to some extent weakened by the decrease in the reduced mass of vibrations, from about 4-7 units for low-frequency vibrations (below about 900 cm$^{-1}$), to 1 unit for high-frequency stretching vibrations that involve hydrogen atoms.

Transformation of Eq. (12) facilitate the calculation of the absolute value of the geometry change for a given normal coordinate in Cartesian coordinates, given by Eq. (13).

$$\left|D^{\mathrm{Cart}}_{\mathrm{ex}\ i}\right| = \sqrt{\frac{hc}{2\pi^2}\frac{I(v_{i\ 0}^{\ 1})}{\mu_i \nu_i}} \qquad (13)$$

The dependence of $D_i^{\mathrm{Cart}}$ on the square root of inetsity in Eq. (13) makes the relative error of displacement parameters in Cartesian coordinates being half of the relative error of experimental band intensities.

The magnitude of geometry changes for the individual normal coordinates included in the fitting of FC factors can be evaluated quantitatively by analyzing the squares of the elements of the vector of geometry changes $(D_i^{\mathrm{Cart}})^2$. That is because they are additive and their sum is equal to the square of the length of this vector and is invariant with respect to orthogonal transformations of normal coordinates.

The sum of squares of the elements of the $D_i^{\mathrm{Cart}}$ vector included in the fitting of FC factors is denoted by the square of length (norm) of the $\vec{D}^{\mathrm{Cart}}_{\mathrm{ex\,FCfit}}$ vector. This norm divided by the norm of the entire vector of geometry changes $D_i^{\mathrm{Cart}}$, which is included in the denominator in Eq. (14). The experimental intensities for the fundamental transitions $\upsilon_i$=0→1 divided by the product of reduced mass and frequency can be substituted in this equation instead of the squares of elements of the $D_i^{\mathrm{Cart}}$ vector.

$$\frac{\left\|\vec{D}^{\mathrm{Cart}}_{\mathrm{ex\,FCfit}}\right\|^2}{\left\|\vec{D}^{\mathrm{Cart}}_{\mathrm{ex\,Total}}\right\|^2} = \frac{\sum\limits_{i=FC\,fit}\left(D^{\mathrm{Cart}}_{\mathrm{ex}\ i}\right)^2}{\sum\limits_{j}\left(D^{\mathrm{Cart}}_{\mathrm{ex}\ j}\right)^2} = \frac{\sum\limits_{i=FC\,fit}\frac{I(v_{i\ 0}^{\ 1})}{\mu_i\nu_i}}{\sum\limits_{j}\frac{I(v_{j\ 0}^{\ 1})}{\mu_j\nu_j}} \qquad (14)$$

The contributions of the squares of reduced displacement parameters $\Delta_i$ in individual normal coordinates to the total sum of their squares (marked as **Δ** or ▲) and analogous contributions of squares of elements of the $D_i^{\mathrm{Cart}}$ vector(marked as ○ or ●) in their total sum of squares are shown in Fig.22.

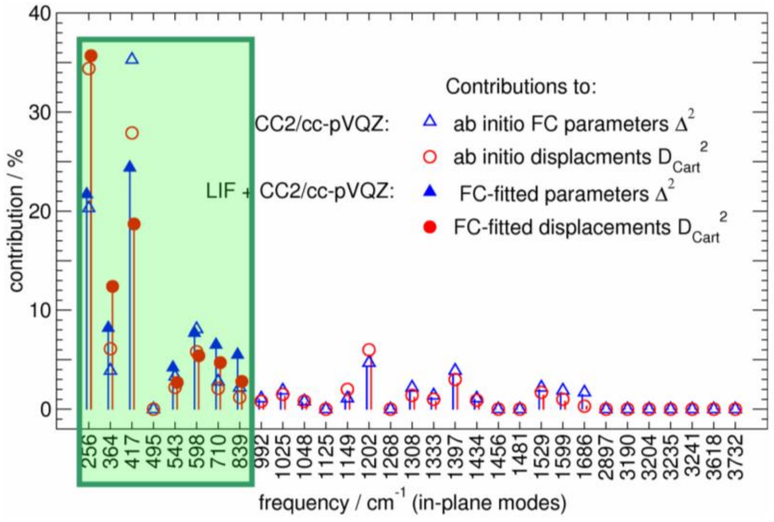

**Fig. 22.** [H7] Contributions of the squares of the reduced displacements $\Delta_i$ and the squares of Cartesian displacements $D^{\mathrm{Cart}}_{\mathrm{ex}\ i}$ to the sum of intensities of fundamentals and to the total geometry changes, respectively. All values are normalized to unity (*ab intio* results: Δ,○; FC-fitted values: ▲,●). The green rectangle marks modes included in the FC fitting of geometry changes.

In Fig.22 we can trace the influence of $1/\mu_i\nu_i$ factor in Eq. (14). This factor causes that the contribution of low frequency vibrations (>500 cm$^{-1}$ and of reduced masses $\mu_i$ = 3-4 units, typically) to the sum of squares of the Cartesian geometry changes is clearly greater than their contribution to the sum of squares of the reduced displacement parameters. For higher frequency vibrations the opposite effect usually takes place. The latter case also occurs for the 417 cm$^{-1}$ mode because of its very large reduced mass (about 7 units), which is only comparable to the reduced mass for the carbonyl stretching ($\nu_{\mathrm{C=O}}$ = 1686 cm$^{-1}$).

The seven displacement parameters subject to optimization[H7] (for vibrations of frequencies below 900 cm$^{-1}$ shown in the green rectangle in Fig.22, excluding the 459 cm$^{-1}$ mode with zero displacement) accounts for more than 80% of the sum of squares of Cartesian geometry changes, and the length of the $\vec{D}^{\mathrm{Cart}}_{\mathrm{ex\,FCfit}}$ vector composed of these components comprises more than 0.9 of the total length of the $\vec{D}^{\mathrm{Cart}}_{\mathrm{ex\,Tot}}$ vector of geometry changes. Thus 7 out of 31 components (number of totally-symmetric vibrations) of this vector represents a dominant contribution to total changes in equilibrium geometry of the molecule. Moreover, the total contribution of only 3 most important normal coordinates (for oscillations: 256 cm$^{-1}$, 364 cm$^{-1}$ and 417 cm$^{-1}$) accounts for about 65% of the sum of squares of geometry changes, and the length of the vector composed of these components accounts for about 0.8 of the length of total geometry changes[H7].

Potential energy distribution (PED) indicate that the vibrations contributing the most to the geometry changes mainly correspond to rocking motions of substitutes as a whole, with some contribution of bending deformations within substitutes[H4,H7]. Analysis of PED for 256 cm$^{-1}$ vibration shows 55% contribution of rocking motion of COOH group and 20% contribution of bending of C–C=O angle. The 364 cm$^{-1}$ mode consists of: 40% contribution of $NH_2$ rocking with respect to the aromatic ring. With another choice of internal coordinates used for the calculation of potential energy distribution PED, the first two vibrations correspond essentially to the change in length of the O···H hydrogen bond, which has more than 80% contribution of PED in both oscillations. In turn, the mode 417 cm$^{-1}$ consists of simultaneous rocking motions of both substitutes in the same direction ($NH_2$ rocking: 33% and COOH rocking: 22%), which hardly change the length of the hydrogen bond. Whereas with an alternative choice of internal coordinates in PED calculations this oscillation has the dominant contribution (PED: 75%) of the deformation of the chelate ring, formed from both substituents through the hydrogen bond.

The contribution of geometry changes related to normal coordinates optimized by fitting to the experimental intensities and geometry changes for other normal coordinates resulting directly from quantum-chemical calculations were calculated explicitly for individual internal coordinates[H7]. These results indicate that the changes in length of the N–H···O hydrogen bond and the changes in skeletal angles in the molecule are determined mainly via fitting of the FC factors to the experimental data. Whereas the changes of bond length in $\pi$-electronic system depend largely on the FC factors resulting directly from the quantum-chemistry calculations and not verified on the basis of the experimental data. This is due to the fact that almost all normal coordinates included in optimization of FC factors have dominant contributions of valence angle deformations in the potential energy distribution PED[H4,H7], and only the vibration with experimental frequency 713 cm$^{-1}$ (726 cm$^{-1}$ CC2) has a dominant contribution of bond stretching. A few remaining bands of low intensities are assigned to stretching vibrations with frequencies above 900 cm$^{-1}$ and are present in a very congested spectral range in the LIF spectrum. Moreover, they may be subject to noticeable mode mixing upon the excitation. These bands have not been taken into account in the fitting of displacement parameters[H7], because the relevant vibrations have a small total contribution in the geometry changes and additionally, the above mentioned factors may cause the occurrence of phenomena interfering with the relation between the band intensities and the displacement parameters.

Geometry changes determined by fitting of FC factors to the experimental spectra have similar values, regardless of the use of normal vibrations calculated by CC2 or TDDFT. Noticeable discrepancies between the overall estimates of geometry changes are mainly due to discrepancies between the CC2 and TDDFT methods for the component of geometry changes related to the displacement parameters for the remaining 24 normal vibrations, that were not included in the procedure for matching the FC factors to the experimental data. Nevertheless, the displacement parameters for the remaining 24 normal coordinates carry important, although dispersed, information concerning geometry changes, especially with regard to changes of bond lengths in the π-electronic system. Moreover, they are important, because of the compensation of errors in the calculation of FC factors using Cartesian coordinates, instead of using curvilinear internal coordinates. For both reasons I kept the values of FC factors for the remaining vibrations unchanged.

### *Errors induced by the use of Cartesian coordinates instead of curvilinear internal coordinates*

In order to estimate the errors resulting from the use of Cartesian coordinates instead of curvilinear internal coordinates, I carried out the following analysis[H7] of transformations used in the calculation of FC factors and modeling of the geometry changes. To summarize, it should be noted that the transformations described in Equations (8)-(11) describe a closed cycle of transformations consisting of three stages. In the first stage, the reduced displacement parameters in normal coordinates and Franck-Condon factors were calculated from the following results of quantum chemistry calculations: the equilibrium geometries of the molecule in both electronic states or rather their differences and the computed normal vibrations. In the second stage, the least squares method was used to fit the displacement parameters in order to achieve optimal consistency of the modeled band intensities with the experimental values. In the final stage, the geometry changes upon the electronic excitation were calculated on the basis of the optimized values of the displacement parameters. Owing to the above, the errors of the determined geometry changes, caused by the use of Cartesian coordinates in the closed cycle of calculation described above, would cancel exactly if the fitting to the experimental data did not change the initial values of the geometry changes calculated with quantum chemistry methods. In such a case, the compensation of geometry change errors would be complete and accurate, although the use of Cartesian coordinates could cause inaccuracies in the calculated FC factors and the modeled intensities of vibronic bands. The presented reasoning indicates that the errors of geometry changes determined by fitting FC factors, caused by the use of Cartesian coordinates do not depend on the total value of geometry changes but only on the magnitude of the corrections to those changes, with respect to their initial values (calculated preliminary with quantum chemistry methods).

Calculations of displacement parameters in Cartesian coordinates are based on factorization of the changes in equilibrium geometry using finite displacements of atoms in particular normal vibrations. The errors are induced because the factorization of curvilinear displacements associated with angular deformations is approximated with the Cartesian finite displacements of atoms in particular normal vibrations. These displacements are tangential to the actual curvilinear displacements specific for bending vibrations. In case of analytical normal vibrations they are exactly tangential. In case of numerical calculations of normal vibrations based on numerical differentiation of Hessian, they remain a very good approximation of these tangents, because a typical numerical step for the displacements of atoms in these calculations is of the order of magnitude $10^{-3}$ Å, which corresponds to the distortion of valence angles of roughly 0.05°. The above factorization causes concerning the erroneous lengthening of the valence bonds due to the linear approximation of the angular deformations. These errors must then be compensated by erroneous corrections to the displacement parameters for the stretching vibrations involving these bonds. This generates the errors which are included in the total values of FC factor and band intensities for stretching vibrations. Trigonometric considerations[H7] lead to a quantitative estimation of these errors caused by the distortion of angle $\alpha$ by value $\Delta\alpha$ (for the angle formed by the group of atoms B–A–B'). Erroneously elongated bond reaches the length $R'$ given by Equation (15), where $R$ is the real length of this bond.

$$R'(\Delta\alpha) = \frac{R}{\cos\Delta\alpha} \tag{15}$$

According to this equation, the error of bond length: $\Delta R_{\mathrm{err}}(\Delta\alpha) = R'(\Delta\alpha) - R$, for typical bonds in the aromatic system, of length 140 pm, and for $\Delta\alpha = 1°$ is negligible and amounts only to 0.021 pm[H7]. But the error increases approximately quadratically with the increase of $\Delta\alpha$ and for $\Delta\alpha = 10°$ it reaches the value about a hundred times greater: $\Delta R_{\mathrm{err}}(10°) = 2.16$ pm, which is already a significant amount. However, such a magnitude of the error occurs only if the deformation of the angle by $\Delta\alpha$ causes a curvilinear displacement of only one angle arm, and the other arm remains stationary. This is the case if we consider the motion of hydrogen atom or other light atom (and approximately also the motion of the light substituent) in respect to the rigid molecular skeleton. The smallest errors arise if the deformation of the angle by $\Delta\alpha$ causes two equal displacements of both atoms (or groups of atoms) B and B' by ½$\Delta\alpha$. Then, because of approximately quadratic dependence of $\Delta R_{\mathrm{err}}$ on $\Delta\alpha$, the lengths of both bonds are subject to errors, which are however 4 times smaller than in the previous case. Because the corrections of the values of valence angles calculated during the fitting of FC factors do not exceed 1° for the FC fit: LIF+CC2 and 1.7° for the FC fit: LIF+TDDFT, the maximum errors resulting from such a $\Delta\alpha$ correction are 0.021 pm and 0.061 pm, respectively. Even taking into account the accumulation of errors due to deformations of several valence angles, the resultant errors shall not exceed 0.05 pm for the FC fit: LIF+CC2 and 0.15 pm for the FC fit: LIF+TDDFT. The accumulation of errors could be significant, for molecules consisting of long and flexible aliphatic chains but not for the investigated molecule built on a fairly rigid aromatic skeleton. Thus, these errors remain insignificant and much smaller than both the experimental errors and the variation of results due to the use of various basis sets in these modeling.

Another important issue is the influence of errors caused by the use of Cartesian coordinates, on the modeled values of FC factors and intensities of vibronic bands. On the one hand, the deformations of valence angles, typically up to 5° for skeletal angles and up to a maximum of 7.4° (for $C_2$–$C_1$–N) are significant and may seem to induce significant errors of FC factors. On the other hand, however, geometrical considerations indicate that the actual curvilinear displacements of atoms are roughly twice as small, so instead of maximum errors of bond length, of values 0.53 pm in the first case and 1.2 pm in the second, errors even 4 times smaller can be expected. Moreover, noticeable values of FC factors and intensities of bands associated with skeletal stretching vibrations, arise only as a result of changing the length of skeletal bonds almost by an order of magnitude larger, namely around 5 pm. Thus erroneous elongation of bonds even by 0.5 pm does not cause any significant changes of bands intensities in the modeled spectra.

## II.5. SUMMARY AND CONCLUSIONS

Owing to the complementary and synergistic use of advanced research methods, both experimental and theoretical, I have conducted studies on the vibrational structure of the LIF spectra of anthranilic acid and its deuterated derivatives and I determined the equilibrium geometry changes accompanying the electronic excitation. The obtained results and research achievements can be summarized in three groups.

***Experimental results and achievements***

1. Recording of detailed spectral data in the laser-induced fluorescence spectra LIF of anthranilic acid molecules and its isotopomers, cooled to cryogenic temperatures in supersonic molecular beam.
2. The distinction of the vibronic bands belonging to the spectrally overlapping $S_0 \rightarrow S_1$ transition bands of the anthranilic acid monomer, its dimer and its 8 isotopomers.
3. Investigation of anharmonic effects of significant importance for identification of vibrinic bands in the studied spectra.
4. Measurements of reliable band intensities, carried out owing to: reduction of the scattering of the laser beam, improvement of signal-to-noise ratio in the recorded spectra, reduction of saturation effects, and normalization of the fluorescence signal with respect to the systematic changes and fluctuations in intensity of the laser beam.

***Theoretical results and achievements***

1. Calculations of the equilibrium geometry and normal vibrations for a molecule in the excited electronic state, using advanced quantum chemistry methods: TDDFT and CC2, taking into account the multi-configurational nature of the excited state, electronic correlation and the peculiar features of the intramolecular hydrogen bond.
2. Modeling of Franck-Condon factors in the 1-dimensional and the multi-dimensional model, based on calculations using the TDDFT and the CC2 methods with a series of basis sets: (aug)-cc-pVXZ(X=D,T,Q).
3. Introduction of equation describing changes in the frequency of normal vibrations due to isotopic exchange, as a function of the reduced mass of vibrations and the amplitude of displacements of individual atoms in particular vibrations.
4. Application of the orthogonal matrix of the projection of normal coordinates (being an analogue of the Dushinsky matrix) for the mutual identification and quantitative comparison of normal vibrations computed with various quantum chemistry methods or for isotopically substituted molecules.

***Results and achievements obtained owing to complementary and synergistic application of both experimental and theoretical research methods***

1. Obtaining quantitatively consistent modeling of FC factors and estimation of the changes in equilibrium geometry upon the excitation, based on experimental band intensities in the LIF spectra, and normal vibrations computed with quantum chemistry methods.
2. The study of variability of the modeling results of the changes in the equilibrium geometry caused by the use of: various models of FC factors, various quantum chemistry methods and a series of basis sets.
3. Estimation of contributions of the experimental band intensities to the changes in the equilibrium geometry and assessment of the completeness of the modeled changes.
4. discussion of errors caused by inaccuracies in experimental results, and carrying out the modeling in Cartesian coordinates, instead of using curvilinear internal coordinates.

In the LIF spectra, the activity of 10 plane normal vibrations of the anthranilic acid molecule in the excited state $S_1(\pi\rightarrow\pi^*)$ was detected, of which only 4 were previously detected and identified[22,25]. The predominant cause of the activity of the totally-symmetric (in-plane) oscillations in the LIF spectra are the differences in the equilibrium geometry of the molecule between the ground and the excited state.

In order to verify the identification of bands in the LIF spectra, I have studied the anharmonic corrections as well as the isotopic effects resulting from the deuteration of $NH_2$ and COOH groups in the anthranilic acid molecule. The isotopic shifts for normal vibrations due to isotopic substitution of hydrogen atoms in various positions allowed to derive an equation describing the changes in the frequency of normal vibrations due to isotopic substitution. Additionally, I have carried out studies of subtle effects related to the shifts of adiabatic transition due to deuteration of the molecule in various positions. They provided the experimental data[H5] which, in combination with the quantum chemistry computations and the modeling of zero vibration energy correction ZPE, showed that the anthranilic acid molecule is dynamically planar already in the ground state, due to the energy of zero vibrational level and a very low barrier for the amino group inversion motoin[37].

The experimental bands intensities in the LIF spectra, supported by vibrations computed with quantum chemistry methods, have provided the base for modeling of the changes in the equilibrium geometry of the molecule due to the electronic excitation. The results of quantum chemistry calculations as well as the modeling of FC factors and geometry changes based on experimental spectra indicate that the greatest change in equilibrium geometry concerns the shortening of the intramolecular hydrogen bond. The aim of quantum chemistry calculations and modeling of FC factors was to obtain a reliable estimation of the magnitude of the geometry changes, being an important research problem, from the point of view of quantum chemistry as well as experimental and theoretical molecular spectroscopy. Especially since in the previous studies, the magnitudes of these changes had been, predicted using various quantum chemistry methods, had shown substantial discrepancies with each other.

Modeling of FC factors on the basis of quantum-chemical calculations showed that calculated band intensities, as well as values of equilibrium geometry changes, are drastically underestimated in HF and CIS[H2,H3] methods and clearly underestimated in DFT and TDDFT(B3LYP)[H3,H7]. It has therefore become appropriate to use the more accurate CC2 method, which is a perturbative approximation to the CCSD coupled cluster method, and in addition, to perform the fitting of FC parameters, in order to achieve consistency with the experimentally determined band intensities in the LIF spectra. The latter allowed for the determination of FC parameters based on experimental results. Then, with the help of normal vibrations computed via vibrational analysis with quantum chemistry methods, geometry changes in Cartesian coordinates and changes in bond length and valence angles were calculated[H3,H7].

According to my research it was found that the most reliable estimation for the shortening of the distance between the amino hydrogen atom and the oxygen atom is $\Delta R(\mathrm{O}\cdots\mathrm{H}) = -31\ \mathrm{pm}\ \pm 1{,}5\ \mathrm{pm}$, to around 1.60 Å[H7] in the excited state. This value was established on the basis of the fitting of Franck-Condon factors to the intensity of vibronic bands in the LIF spectrum, using normal vibrations calculated by CC2 method (FC fit: LIF+CC2H7). This value was determined in a multidimensional model of Franck-Condon factors (MFC), taking into account the variability of the results due to calculations in a series of basis sets and errors of the experimental intensity measurement. However, the fits obtained with the aid of DFT and TD-DFT[H3,H7] calculations predict values in the range –(29-32) pm (FC fit: LIF+DFT).

The shortening of the hydrogen bond is facilitated mainly by the changes in valence angles, which reaches 7.5° for C2-C1-N and for other angles approaching 5°. They mainly concern the rocking motions of the substitutes and the deformation of the substitutes as well as the deformation of the aromatic ring. Whereas, the changes of bond alternations in the π-electron system reach 5 pm. Most importantly, noticeable strengthening concerns the π-electronic coupling of the carboxylic group with the aromatic ring, which is much stronger in the $S_1$ excited state than in the ground state. This is evidenced by the clear shortening and strengthening of the C–COOH bond, whose length approaches 1.43 Å in the excited state, and reaches the value of the longer bonds in the aromatic ring.

Achieving the above consistency of results is a noticeable achievement of modelling of changes in equilibrium geometry by fitting Franck-Condon factors, based on complementary and synergistic use of experimental and theoretical research methods. The most important achievement of the developed approach is obtaining the estimation of geometry changes based on the experimental data, for a polyatomic molecule that consists more than dozen atoms, in which, in spite of significant rigidity of the molecular skeleton, large geometry changes take place, which results from the strengthening of the intramolecular hydrogen bond. Moreover, these estimates are characterized by small discrepancies between the geometric changes determined by fitting of FC factors to the experimental data using theoretically calculated normal vibrations[H7]. These discrepancies are much smaller than the discrepancies between the corresponding values calculated with the quantum chemistry methods[H6].

The proposed methodology gives a consistent estimate of geometry changes, provided that certain criteria are fulfilled. Firstly, performing reliable measurements of intensities of vibronic bands in the laser-induced fluorescence spectrum for molecules isolated from intermolecular interactions and cooled to cryogenic temperatures in supersonic expansion. Secondly, the use of appropriate FC factor models. Thirdly, the use of the relevant, high-level quantum chemistry methods for the calculation of normal vibrations, giving qualitatively adequate description of the excited electronic state as well as the dynamic electronic correlation and the nature of the hydrogen bond in the excited state.

An in-depth analyses of the obtained results of quantum-chemical calculations[H6] and the results of modeling of FC factors and geometry changes[H7] were carried out in order to estimate the reliability and accuracy of the results as well as to examine the magnitude and sources of discrepancies among them. It was found that geometry changes calculated with the CC2 method cover about 90% whereas those calculated with TDDFT method – about 60% of geometry changes determined on the basis of experimental results.

The most accurate and reliable estimation of geometry changes is undoubtedly the results of the fitting of FC factors to the experimental band intensities aided by normal vibrations calculated by CC2 method. This is due to the fact that the CC2 calculation alone gives a quite accurate estimation of the geometry changes, and therefore it is a very good starting point for the FC fitting (FC fit: LIF+CC2)[H7]. Nevertheless, carrying out the FC fitting in order to achieve consistency with the experimental bands intensities, allows to obtain sufficient accuracy of the estimation of geometry changes, also if they are supported by quantum-chemistry calculations with the TDDFT[H6,H7], which takes into account a significant part of electronic correlation at rather low calculation cost.

Discrepancies in the excited-state equilibrium geometries and thus the geometry changes computed using various basis sets with the same quantum chemistry method are noticeable. On the other hand, only a minor dispersion is found between the geometry changes resulting form the of fitting of FC factors supported by normal vibrations calculated with various basis sets. Therefore, for the correct modeling of geometry changes via fitting of FC factors, it is not necessary to use very large basis sets in the calculation of normal vibration.

## II.6. BIBLIOGRAPHY

1 Bloino, J.; Biczysko, M.; Crescenzi, O.; Barone, V. Integrated computational approach to vibrationally resolved electronic spectra: Anisole as a test case. *J. Chem. Phys.* **2008**, *128*, 244105(1-15).

2 Barone, V.; Bloino, J.; Biczysko, M.; Santoro, F.; Fully integrated approach to compute vibrationally resolved optical spectra: from small molecules to macrosystems. *J. Chem. Theory Comput.* **2009**, *5*, 540-554

3 Santoro, F.; Mortaheb, F.; Lepelmeier, J.; Boesl, U.; Heiz, U.; Kartouzian A. High-resolution absorption and electronic circular dichroism spectra of (R)-(+)-1-phenylethanol. Confident interpretation based on the synergy between experiments and computations. *ChemPhysChem* **2018**, *19*, 715 –723.

4 Stuhlmann B , Grassle A , Schmitt M . Determination of the geometry change of 5-cyanoindole upon electronic excitation from a combined franck-condon/rotational constants fit. *Phys Chem Chem Phys* **2014**;*16*:899–905 .

5 Gmerek F , Stuhlmann B , Alvarez-Valtierra L , Pratt DW , Schmitt M . Electronic spectra of 2- and 3-tolunitrile in the gas phase. II. geometry changes from franck-condon fits of fluorescence emission spectra. *J Chem Phys* **2016**;*144*(1–8):084304 .

6 Turchiello, R. F.; Lamy-Freund, M. T.; Hirata, I. Y.; Juliano, L.; Ito A. S. Ortho-aminobenzoic acid as a fluorescent probe for the interaction between peptides and micelles. *Biophys. Chem*. **1998**, *73*, 217–225.

7 Ito, A. S.; Turchiello, R. F.; Hirata, I. Y.; Cezari, M. H. S.; Meldal, M.; Juliano, L. Fluorescent properties of amino acids labeled with ortho-aminobenzoic acid. *Biospectrosopy*, **1998**, *4*, 395–402.

8 Weller, A. Fast reactions of excited molecules. *Prog. React. Kinet. Mech.* **1961**, *1*, 187–197.

9 Heimbrook, L.; Kenny, J. E.; Kohler, B. E.; Scott, G. W. Lowest excited singlet-state of hydrogen bonded methyl salicylate. *J. Phys. Chem.* **1983**, *87*, 280–289.

10 Bisht, P. B.; Petek, H.; Yoshihara, K.; Nagashima, U. Excited state enol-keto tautomerization in salicylic acid: A supersonic free jet study. *J. Chem. Phys.* **1995**, *103*, 5290–5307.

11 Nagaoka, S.; Nagashima, U. Intramolecular proton transfer in various electronic states of otho-hydroxybenzaldehyde. *Chem. Phys.* **1989**, *136*, 153–163.

12 Lahmani, F.; Zehnacker-Rentien, A. Effect of substitution on the photoinduced intramolecular proton transfer in salicylic acid. *J. Phys. Chem. A* **1997**, *101*, 6141–6147

13 Peteanu, L. A.; Mathies, R. A. Resonance Raman intensity analysis of the excited-state proton transfer in 2-hydroxyacetophenone. *J. Phys. Chem.* **1992**, *96*, 6910–6916.

14 Yahagi, T.; Fujii, A.; Ebata, T.; Mikami, N. Infrared Spectroscopy of the OH Stretching Vibrations of Jet-Cooled Salicylic Acid and Its Dimer in S0 and S1. *J. Phys. Chem. A* **2001**, *105*, 10673-10680.

15 Herek, J. L.; Pedersen, S.; Banares, L.; Zewail, A. H. Femtosecond real-time probing of reactions. IX. Hydrogen-atom transfer. *J. Chem. Phys.* **1992**, *97*, 9046–9061.

16 Vener M.V., Scheiner S. Hydrogen bonding and proton transfer in the ground and lowest excited singlet states of o-hydroxyacetophenone. *J Phys Chem* **1995**; *99*: 642–649

17 Sobolewski, A. L.; Domcke, W. Ab initio study of excited-state intramolecular proton dislocation in salicylic acid. *Chem. Phys.* **1998**, *232*, 257–265.

18 Sobolewski, A. L.; Domcke, W. Ab initio potential-energy functions for excited state intramolecular proton transfer: a comparative study of o-hydroxybenzaldehyde, salicylic acid and 7-hydroxy-1-indanone. *Phys. Chem. Chem. Phys.* **1999**, *1*, 3065–3072.

19 Sobolewski, A. L.; Domcke; W. On the mechanism of rapid non-radiative decay in intramolecularly hydrogen-bonded pi systems. *Chem. Phys. Lett.*, **1999**, *300*, 533-539.

20 Stalin, T.; Rajendiran, N. Intramolecular charge transfer associated with hydrogen bonding effects on 2-aminobenzoic acid. *J. Photochem. Photobiol. A: Chemistry* **2006**, *182*, 137–150.

21 Sobolewski, A. L.; Domcke, W. Intramolecular hydrogen bonding in the S1(ππ*) excited state of anthranilic acid and salicylic acid: TDDFT calculation of excited-state geometries and infrared spectra. *J. Phys. Chem. A* **2004,** *108*, 10917–10922.

22 Southern, C. A.; Levy, D. H.; Florio, G. M.; Longarte, A.; Zwier, T. S. Electronic and infrared spectroscopy of anthranilic acid in a supersonic jet. *J. Phys. Chem. A*, **2003**, *107*, 4032–4040.

23 Southern C. A., Levy D. H, Stearns J. A., Florio G. M., Longarte A., Zwier T. S. Spectroscopic Consequences of Localized Electronic Excitation in Anthranilic Acid Dimer. *J. Phys. Chem. A,* **2004,** *108,* 4599-4609

24 Stearns J. A., Das A., Zwier T. S., Hydrogen atom dislocation in the excited state of anthranilic acid: probing the carbonyl stretch fundamental and the effects of water complexation. *Phys. Chem. Chem. Phys.* **2004**, *6,* 2605-2610.

25 Wu, C.; He, Y.; Kong, W. Two-color two-photon REMPI and ZEKE spectroscopy of supersonically cooled o-aminobenzoic acid. *Chem. Phys. Lett.* **2004**, *398*, 351−356.

26 Y. He, C. Wu, W. Kong, A Theoretical and Experimental Study of Water Complexes of m-Aminobenzoic Acid MABA·(H2O)n (n = 1 and 2). *J. Phys. Chem. A*, **2005**, *109*, 748-753.

27 Y. He, C. Wu, W. Kong, Theoretical and experimental studies of water complexes of p- and o-aminobenzoic acid. *J. Phys. Chem. A* **2005**, *109,* 2809-2815

28 Rodrigues N. d.N., Cole-Filipiak N. C., Blodgett K. N., Abeysekera C., Zwier T. S., Stavros V. G. Wavepacket insights into the photoprotection mechanism of the UV filter methyl anthranilate. *Nature Comunications,* **2018,** *9* 5188 1-8

29 Rodrigues N. d.N., Cole-Filipiak N. C., Turner M.A., Krokidi K., Thornton G.L., Richings G. W., Hine N. D., Stavros V. G. Substituent position effects on sunscreen photodynamics: A closer look at methyl anthranilate. *Chem. Phys.*, **2018**, *515*, 596-602.

30 Christiansen O, Koch H, Jørgensen P. The second-order approximate coupled cluster singles and doubles model CC2. *Chem. Phys. Lett.* 1995;243:409–18.

31 Hättig C . Geometry optimizations with the coupled-cluster model CC2 using the resolution-of-the-identity approximation. *J. Chem. Phys*. **2003**; *118*: 7751–61.

32 Köhn A , Hättig C . Analytic gradients for excited states in the coupled-cluster model CC2 employing the resolution-of-the-identity approximation. *J. Chem. Phys*. **2003**; *119*:5021–36.

33 Doktorov, E. V.; Malkin, I. A.; Man'ko, V. I. Dynamical symmetry of vibronic transitions in polyatomic molecules and Franck-Condon principle. *J. Mol. Spectr.* **1975**, *56*, 1-20.

34 Gruner, D.; Brumer, P. Efficient evaluation of harmonic polyatomic Franck-Condon factors. *Chem. Phys. Lett.* **1987**, *138*, 310-314.

35 Ruhoff, P. T. Recursion relations for multidimensional Franck-Condon overlap integrals. *J. Chem. Phys.* **1994**, *186*, 355-374.

36 Ruhoff, P. T.; Ratner, M. A. Algorithms for computing Franck-Condon overlap integrals. *Int. J. Quant. Chem.* **2000**, *77*, 383-392.

37 Andrzejak, M.; Kolek, P. Theoretical modeling of deuteration-induced shifts of the 0−0 bands in absorption spectra of selected aromatic amines: The role of the double-well potential. *J. Phys. Chem. A*, **2013**, *117*, 12770–12782.

38 Maciel, B. C. M.; Chaudhuri, P. An ab initio quantum chemical characterization of structure and vibrational spectra of anthranilic acid. *Int. J. Quantum Chem*. **2011**, *111*, 1709−1718.

39 Yoshida H.; Ehara A.; Matsuura H. Density functional vibrational analysis using wavenumber-linear scale factors. *Chem. Phys. Lett*. **2000**, *325*, 477−483.

40 Heckert, M.; Kállay, M.; Tew, D. P.; Klopper, W.; Gauss, J. Basis-set extrapolation techniques for the accurate calculation of molecular equilibrium geometries using coupled-cluster theory. *J. Chem. Phys*. **2006**, *125*, 044108

# III. OTHER ACHIEVEMENTS

Presentation of teaching and organizational achievements
as well as achievements in popularization of science or art

## III.1. CONSTRUCTION AND UPGRADE OF THE INSTRUMENTATION FOR THE LASER SPECTROSCOPY IN SUPERSONIC MOLECULAR BEAM

### *III.1.1. UPGRADE OF THE INSTRUMENTATION FOR RECORDING OF THE LIF SPECTRA*

I have carried out an upgrade of the apparatus for recording of the laser-induced fluorescence spectra LIF in supersonic molecular beams, located in the Department of Physical Chemistry and Electrochemistry at the Faculty of Chemistry of the Jagiellonian University (Kraków, Poland). The modernization conducted in the period 2008-2011 included the following tasks.

1. Replacement of the experiment control and signal processing system based on CAMAC cards from the 1980s with a modern control system based on fast digital signal processing processors (DSP) and ATMega microcontrollers.
2. Integration of the new dedicated tunable second harmonic generator (SHG) based on a high-quality BBO ($\beta$-Ba(BO$_4$)$_2$, $\beta$-barium borate) crystal of non-linear optical properties with the existing experimental setup. This part of modernization was carried out as part of the ATOMIN project *"Study of atomic-scale systems: exact sciences for innovative economy"* POIG.02.01.00-12-023/08.

### *III.1.2 CONSTRUCTION AND LAUNCH OF THE INSTRUMENTATION FOR RECORDING OF THE LASER-INDUCED FLUORESCENCE EXCITATION SPECTRA LIF AND THE DISPERSED FLUORESCENCE SPECTRA IN SUPERSONIC MOLECULAR BEAM*

In the period 2010-2015 I designed, built and put into operation the equipment for studying laser-induced fluorescence excitation spectra LIF and single-vibronic-level dispersed fluorescencespectra in a supersonic molecular beam (supersonic free jet). A general view of the apparatus is shown in Figure 23, while the block diagram of the apparatus is shown in Figure 24.

It should be mentioned that this is a unique apparatus in Poland, because the apparatus for laser spectroscopy in supersonic molecular beams is (to my knowledge) present in only four scientific institutions in the country: 1) the Institute of Physical Chemistry of the Polish Academy of Sciences in Warsaw (Department of Photochemistry and Spectroscopy); 2) the Faculty of Chemistry of the Jagiellonian University in Cracow (Department of Physical Chemistry and Electrochemistry); 3) the Faculty of Physics, Astronomy and Applied Computer Science of the Jagiellonian University (Institute of Physics, Department of Photonics); 4) the College of Natural Sciences of the University of Rzeszow (Centre for Innovation and Transfer of Natural Science and Engineering Knowledge of the University of Rzeszów, Institute of Physical Sciences) built by me.

This equipment is part of the scientific and research equipment of the Molecular Spectroscopy Lab, which is a part of Centre for Innovation and Transfer of Natural Science and Engineering Knowledge of the University of Rzeszów *(Uniwersyteckie Centrum Innowacji i Transferu Wiedzy Techniczno-Przyrodniczej CIiTWTP).* It was financed as a part of the project: The European Regional Development Fund in the period 2005-2013 within the framework of the Carpathian Regional Operational Programme (RPPK.01.03.0 0-18-0 01/10).

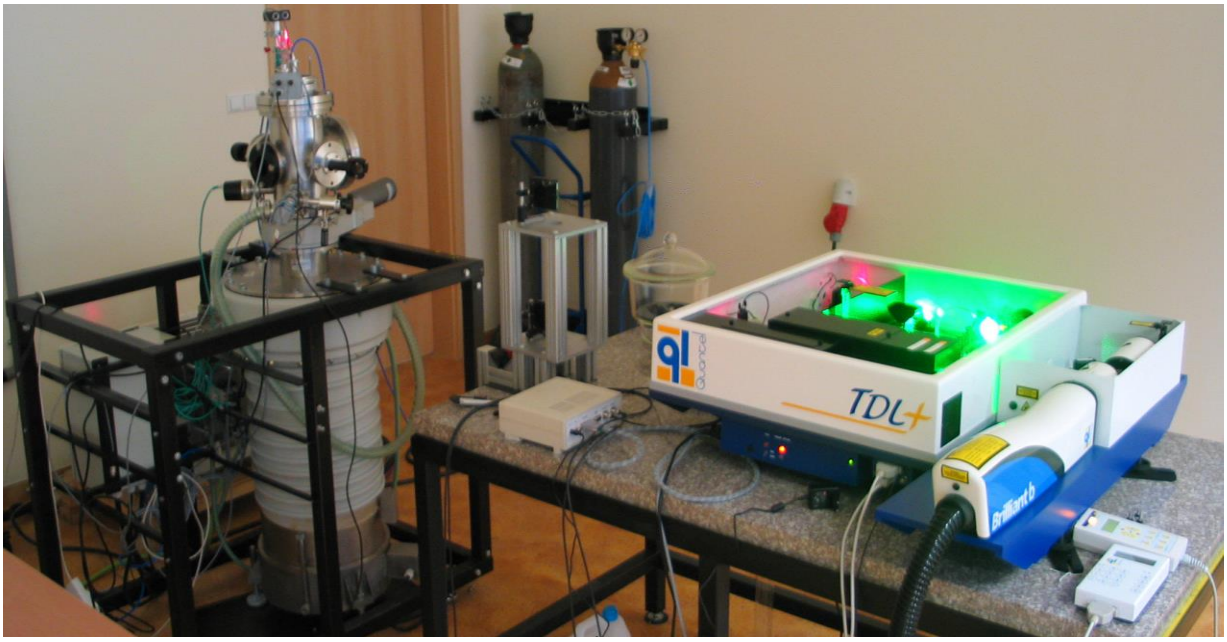

**Fig.** 23 The instrumentation for the recording of the LIF and Dispersed Fluorescence spectra in the supersonic molecular beam.

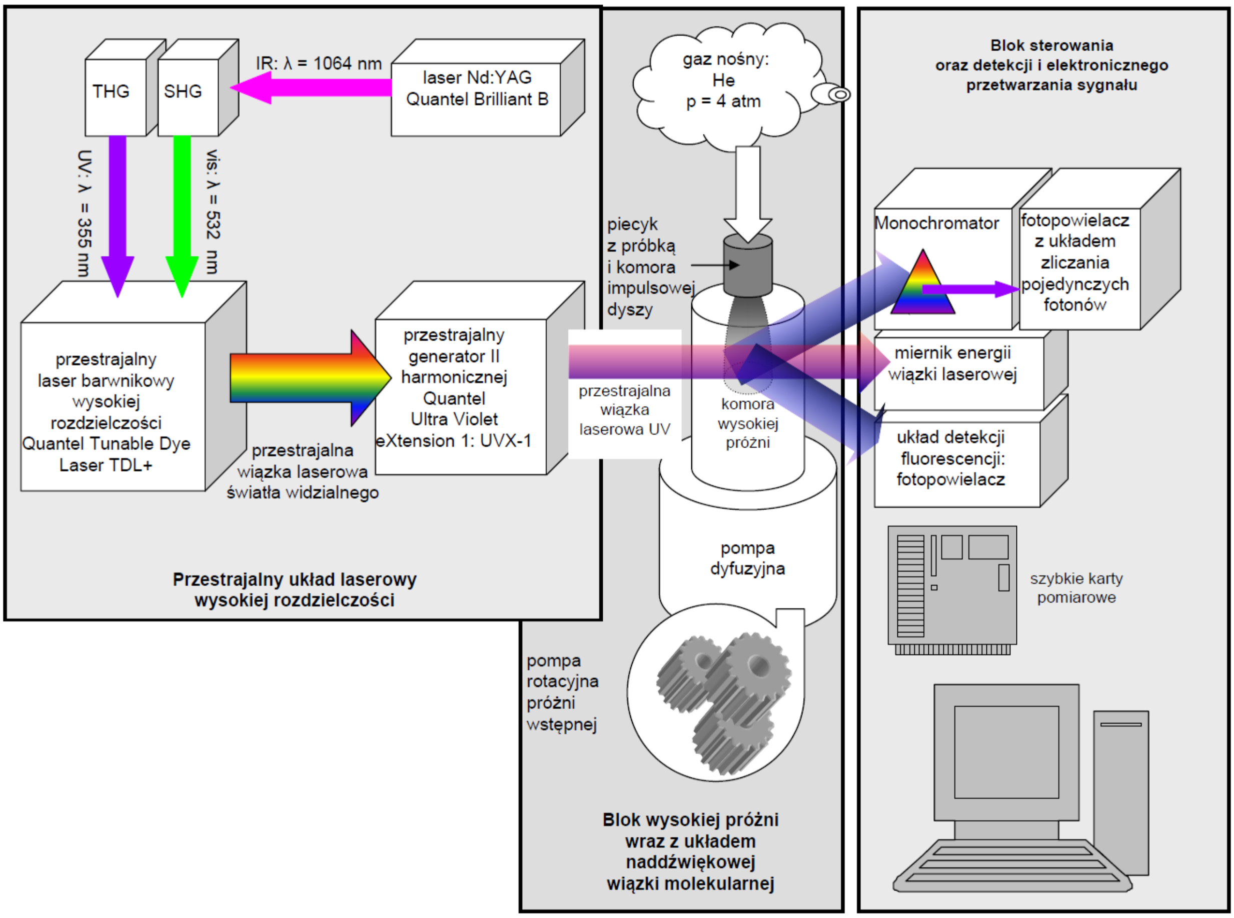

**Fig. 24.** Block diagram of the equipment for recording of the LIF fluorescence excitation spectra and dispersed fluorescence spectra in the supersonic molecular beam.

Based on my previous experience in the field of laser spectroscopy and high-vacuum technology and supersonic molecular beams, I designed an apparatus for spectroscopic studies of molecules cooled to cryogenic temperatures and isolated from intermolecular interactions by expansion of gas in the supersonic jet. Then, in cooperation with manufacturers and suppliers of laser system, high-vacuum instrumentation as well as the electronic control and measurement devices, I took part in the formulation of the detailed design of this equipment. I carried out this task taking into account the current information on the technical capabilities and options of currently available types of individual devices, and their prices within the available budget.

The description of the assembled equipment is included below along with brief information concerning the required parameters and criteria for choosing the most important types of individual devices that can be used in the described apparatus, as well as the choice of the specific technical options that were finally implemented.

***High-vacuum system with the supersonic molecular beam unit***

The part of the equipment designed and manufactured individually for a specific version of the experiment is a high vacuum block with supersonic jet nozzle and sample dosing system (Fig. 25). In order to obtain supersonic expansion conditions, it is necessary to maintain high vacuum conditions in the vacuum chamber at a pressure below $10^{-3}$ or $10^{-4}$ millibar (hPa). A vacuum chamber with a volume of about 10 $dm^3$ has been constructed and equipped with two quartz optical windows to introduce the laser beam and two large-diameter windows at right angles to the laser beam to collect the fluorescence signal.

**Fig. 25.** High vacuum system with supersonic molecular beam unit: on the left, the vacuum chamber mounted on the diffusion pump, on the right, a top view of the cylindrical head with sample furnace and supersonic jet valve.

The sample dosing unit, together with the supersonic jet nozzle, is mounted inside a cylindrical head, which is inserted from the top into the vacuum chamber (Fig. 25 on the right). The carrier gas, injected into the vacuum chamber through a narrow nozzle with an pulse valve, forms a supersonic jet directed directly towards the diffusion pump to facilitate pumping the injected gas, avoiding reflections from the chamber walls. The pulse valve is equipped with a 6 cm long needle, equipped with exchangeable Teflon tips, enabling operation at temperatures up to approx. 300°C, and metal tips – resistant to much higher temperatures, as well as a few exchangeable nozzles with a diameter of 0.3-1.5 mm. A sample furnace is located near the nozzle. The furnace as well as the nozzle outlet and the space where the sample vapour is mixed with the carrier gas are heated electrically and thermostatized independently of each other. The electromagnetic drive of the impulse valve is placed behind a thick wall in which the cooling liquid circuits are placed. This design allows the pulse valve to operate without failure in a wide temperature range, from room temperature up to about 500°C. In order to eliminate most of the impurities from the carrier gas, especially traces of water vapour, which easily forms complexes with the molecules of the sample, helium refrigerated with liquid nitrogen trap was used as the carrier gas.

In order to maintain the high-vacuum conditions necessary to generate the supersonic jet, the vacuum chamber is pumped by a high power pump system: a diffusion pump with a pumping speed of 6000 dm$^3$/s backed by a rotary pump with a pumping speed of 65 m$^3$/h.

The feasible use a turbomolecular pump of a sufficiently high pumping speed as a high-vacuum pump, would be much more expensive. Moreover, the turbo pump would be exposed to strong pulses of gas pressure and damage due to the possibility of unstable operation of the impulse valve injecting supersonic jet, especially at high temperatures. A single-stage pumping system based on a Root mechanical pump, providing a vacuum of $10^{-3}$ or $10^{-4}$ millibar at best, would be highly resistant to strong gas pulses. However, this solution would also be much more expensive than the implemented system.

***Tunable high-resolution laser system***

The investigations of the fluorescence excitation spectra in the supersonic molecular beams are among the methods of high-resolution optical spectroscopy. Conducting them in the extremely diluted medium, which is the supersonic beam expanding in a high-vacuum chamber, requires the use of a laser source of light or UV radiation. These sources must meet very high requirements for the spectral and geometric parameters of the emitted light beam which ensure continuous tuning of the radiation wavelength and high surface energy density in the cross-section of the beam.

The laser system used is shown in Figure 26. As a high-resolution tunable laser, the Quantel Tunable Dye Laser TDL+ (Fig. 26) was used, equipped with two interchangeable diffraction grating (with the groove density of 1800 and 2400 per millimetre). For the optical pumping of this laser the Nd:YAG Quantel Brilliant-B laser we used, equipped with 2nd harmonic generator SHG ($\lambda$=532 nm) and 3rd harmonic generator THG ($\lambda$=355 nm), shown on the left side on Fig. 26.

**Fig. 26** Tunable high resolution laser system. On the left: the head of the Nd:YAG pumping laser, equipped with 2nd and 3rd harmonic generators: SHG and THG. On the right: the tunable high resolution dye laser, equipped with the tunable 2nd harmonic generator, UVX-1.

The configuration of the laser system described above enables tuning in the entire spectral range of visible light. To facilitate tuning of the laser system in the UV range, the tunable second harmonic generator (Ultra Violet eXtension-1, UVX-1) integrated with the dye laser is used, equipped with three interchangeable BBO crystals to cover the spectral range λ=220-380 nm. The laser system configured in this way generates a high-resolution laser beam with a spectral bandwidth of 0.06-1.8 $cm^{-1}$ (depending on the spectral range) in a broad spectral range (220-780nm).

Other feasible laser system configurations, using non-linear optical frequency mixing methods, using two laser beams: a tunable dye laser beam and a pumping laser beam, would require a much more expensive system, which would increase the cost of the entire laser equipment by about 30-50%. The cost of using a non-linear optical frequency mixing method in a parametric optical oscillator (OPO) instead of a dye laser would increase even further. Important advantages of these laser systems include the availability of a tunable laser light beam and near-infrared (by down conversion process) and higher beam energy in the UV range, as well as for the OPO laser, the availability of a very wide spectral range and the capability of rapid tuning. Nevertheless, despite these advantages I was limited to a simpler laser system that the overall budget allowed.

***Experiment control, detection and electronic signal processing block***

The operation of the equipment for recording LIF and Dispersed Fluorescence spectra in the supersonic molecular beam requires the use of an advanced high-sensitivity detection system, and the synchronization of laser pulses with the pulsed operation of the supersonic jet valve and gating of the electronic signal detection system with nanosecond precision.

For the recording of the fluorescence excitation spectra a gated photomultiplier cooled by Peltier element is used. The signal from the photomultiplier is processed in the integral mode (electric current mode), which combined with precise gating ensures high sensitivity, the capability of recording short signals (5-50 nanoseconds) in a wide dynamic range and the elimination of noise occurring in the long periods between short fluorescence pulses. To normalize the fluorescence signal, taking into account the fluctuations in the energy of the excitation beam the value of the fluorescence signal is divided by the value of the excitation beam energy, measured by the laser beam energy meter.

Single vibronnic level dispersed fluorescence spectra are recorded using the detection system consisting of a monochromator, a photomultiplier and an electronic unit. Since the fluorescence signal after passing through the monochromator has a very low intensity, the photomultiplier and the electronics operate in photon counting mode. Due to the very weak signal, the unavoidable compromise between signal intensity and resolution of the recorded spectra is not fully satisfactory.

## III.2. DESIGN AND ORGANIZING OF THE LABORATORY OF PHYSICOCHEMISTRY AND MOLECULAR MODELING

I organized the Lab of Physicochemistry and Molecular Modelling, which is a part of the Centre for Innovation and Transfer of Natural Science and Engineering Knowledge of the University of Rzeszów (*Uniwersyteckie Centrum Innowacji i Transferu Wiedzy Techniczno-Przyrodniczej" CIiTWTP*) and I am currently the head of this Lab. The Lab was financed from the European Regional Funds, as a part of the project: "University Center for Innovation and Transfer of Technical and Natural Knowledge" as part of The European Regional Development Fund within the framework of the Carpathian Regional Operational Programme for 2005-2013, RPPK.01.03.0 0-18-0 01/10 (*Regionalna Strategia Innowacji Województwa Podkarpackiego na lata 2005-2013*).

The apparatus equipment of the Lab includes instruments for the measurements of optical, spectroscopic and electrochemical properties of samples as well as for the colligative properties of liquids and surface phases. In addition, the Lab is equipped with software for molecular modeling using semi-empirical and ab initio methods of quantum chemistry.

## III.3. DIDACTIC ACHIEVEMENTS

### *AUTHORSHIP OF SCRIPTS AND DIDACTIC MATERIALS*

1. The authorship of the student handbook:
   *„Chemia, skrypt drukowany na potrzeby studentów kierunku Inżynieria Materiałowa"*
   Translation of the title: "*Chemistry, textbook printed for students of Material Engineering*"
   Przemysław Kolek, Uniwersytet Rzeszowski, Rzeszów 2014
   ISBN: 978-83-938523-5-2 (262 pages).
   Type of contribution - author, contribution 100%.

2. Co-authorship of the chapter:
   *„Spektroskopia UV cząsteczek schłodzonych w strumieniu naddźwiękowym"*
   Translation of the title: "*UV spectroscopy of molecules cooled in supersonic molecular jet*"
   (pgs: 165-177), Przemysław Kolek, Katarzyna Pirowska, Jan Najbar.
   Type of contribution – coauthor, contribution 40%

   included in the monograph:
   *„Fotochemia i spektroskopia optyczna. Ćwiczenia laboratoryjne",*
   Translation of the title: *"Photochemistry and optical spectroscopy. Laboratory exercises",*
   Collective work edited by: Jan Najbar and Andrzej Turek,
   Wydawnictwo Naukowe PWN, Warszawa 2009 ISBN: 978-83-01-15977-1

   which is a material for the laboratory course on Advanced Physical Chemistry Methods at the Jagiellonian University.

3. Authorship of didactic materials for lectures and laboratory courses on Chemistry for the major: Material Engineering (*Inżynieria Materiałowa*) at the University of Rzeszów.
   Type of contribution - author, 100%.

4. Co-authorship of didactic materials for lectures and laboratory courses Spectroscopy of Materials (*Spektroskopia materiałów*), authors: Dr Przemysław Kolek, Dr Izabela Piotrowska, Dr Małgorzata Ostrowska-Kopeć, for the major in Material Engineering (*Inżynieria Materiałowa*) at the University of Rzeszów.
   Type of participation - co-author, 33%.

5. Author of didactic materials for lectures, exercises and laboratory courses on Introduction to Spectroscopy (*Wprowadzenie do spektroskopii*), for the major: Diagnostic Systems in Medicine at the University of Rzeszów. Type of participation - author, 100%

### *TEACHING EXPERIENCE AT DOMESTIC AND FOREIGN UNIVERSITIES*

### *Teaching subjects related to chemistry, physical chemistry and molecular spectroscopy*

1. Co-conducting of laboratory course on Physical Chemistry (*Chemia fizyczna*), and after splitting the courses, conducting subjects: Physical Chemistry-I (*Chemia fizyczna-I*) and Physical Chemistry-II ((*Chemia fizyczna-II*) in the Faculty of Chemistry at the Jagiellonian University (Cracow. Poland).

2. Conducting exercises on subjects:
   – *Physical chemistry – exercises* in English
   – *Theoretical chemistry and spectroscopy* – in English
   for the Chemistry degree at the University of Basel (Switzerland).

3. Co-conducting the monographic lecture on Laser Spectroscopy (*Spektroskopia laserowa*) for the specialization: Photochemistry and Spectroscopy (*Fotochemia i Spektroskopia*) at the Faculty of Chemistry of the Jagiellonian University (Cracow, Poland).
4. Co-conducting the laboratory course on Advanced Physical Chemistry Methods (*Zaawansowane metody chemii fizycznej*) for the specialization: Photochemistry and Spectroscopy (*Fotochemia i Spektroskopia*) at the Faculty of Chemistry of the Jagiellonian University (Cracow, Poland).
5. Conducting the courses on Chemistry:

   – lectures,
   – exercises
   – laboratory course

   for the majors:

   – Technical Physics (*Fizyka Techniczna*)
   – Material Engineering (*Inżynieria Materiałowa*)
   – Diagnostic Systems in Medicine (*Systemy Diagnostyczne w Medycynie*)
   – Technical and IT education (*Edukacja Techniczno-Informatyczna*)

   at the University of Rzeszow (Poland).
6. Conducting the courses:

   – lectures,
   – exercises
   – laboratory course

   on subjects related to spectroscopy at the University of Rzeszow (Poland):

   – Molecular spectroscopy (*Spektroskopia molekularna*) for major in Physics,
   – Spectroscopy of materials (*Spektroskopia materiałów*) for major in Physics, and major in Technical Physics and major in Material Engineering,
   – Introduction to Spectroscopy (*Wprowadzenie do spektroskopii*) for major Diagnostic Systems in Medicine.
   – Spectroscopy in biological and chemical research (*Spektroskopia w badaniach biologiczno-chemicznych*) for major in Diagnostic Systems in Medicine.

## III.4. PARTICIPATIONS IN PROJECTS FINANCED WITHIN THE EU STRUCTURAL AND SOCIAL PROGRAMMES

### *III.4.1. DEVELOPMENT OF SCIENTIFIC AND RESEARCH POTENTIAL AND INSTRUMENTATION BASE*

I have participated in the following projects, aimed at developing the scientific and research potential, as well as instrumentation and infrastructure base. These projects were co-financed from European Union funds..

1. Participation in **the ATOMIN project "*Atomic Scale Science For Innovative Economy*"** POIG.02.01.00-12-023/08, prepared and carried out by the researchers of the Faculty of Physics, Astronomy and Applied Computes Science together with the Faculty of Chemistry of the Jagiellonian University, in the period 2009-2012. The Project was carried out by scientific staff of the above faculties and was financed from the European Union program: Operational Programme Innovative Economy, Action 2.1. "*Development of centers with high research potential*".

   Character of participation: contractor, researcher, *In the course of this project I carried out the upgrade and modernization of the apparatus for the measurement of the laser-induced fluorescence excitation spectra LIF in a supersonic molecular beam (described in Section III.1.1), located at the Faculty of Chemistry of the Jagiellonian University Kraków, Poland), Department of Physical Chemistry and Electrochemistry, Group of Photochemical and Luminescence Research, which was carried out within the funds allocated for the development and modernization of the apparatus of the Laboratory of Photochemistry and Fast Kinetic Techniques.*

2. **Participation in the project "*Centre for Innovation and Transfer of Natural Science and Engineering Knowledge of the University of Rzeszów*"** financed by the European Union Regional Development Funds, within the framework of the Carpathian Regional Operational Programme (RPPK.01.03.0 0-18-0 01/10) located at the University of Rzeszów (Poland).

   Character of participation: contractor, researcher.

   A) A specialist responsible for designing and launching the set of instrumentation for the laser spectroscopy in supersonic molecular beam, as a part of the Molecular Spectroscopy Lab in the Materials Spectroscopy Laboratory.

   *The course of this project is described in Section III.1.2*

   B) A specialist responsible for designing and start-up of the Lab of Physicochemistry and Molecular Modelling within Materials Spectroscopy Laboratory and currently head of this Lab.

   *I organized the Lab of Physicochemistry and Molecular Modelling described in Section III.2.*

### III.4.2. DEVELOPMENT OF DIDACTIC POTENTIAL

I have participated in the following projects, aimed at developing the didactic potential. These projects were co-financed from European Union Social Funds.

1. Participation in the program ***„UR – Nowoczesność i Przyszłość Regionu”* ("*UR – Modernity and Future of the Region*"),** implemented at the University of Rzeszów and financed by the European Social Fund, under the Human Capital Operational Programme, Action 4.1 *„Wzmocnienie i rozwój potencjału dydaktycznego uczelni oraz zwiększenie liczby absolwentów kierunków o kluczowym znaczeniu dla gospodarki opartej na wiedzy*” ("*Reinforcement and development of the didactic potential of the university and increasing the number of graduates of faculties of key importance to the knowledge-based economy*") of Priority IV „*Szkolnictwo wyższe i nauka*”("*Higher education and science*"). Project duration: 2010-2016.

   Character of participation in the project:

   a) author of the chemistry handbook for students,
   b) author of didactic materials on chemistry,
   c) co-author of didactic materials on spectroscopy of materials,
   d) participant in a professional English language course within the framework of the action „*Budowa potencjału dydaktycznego Uniwersytetu Rzeszowskiego na poziomie europejskim*” ("*Building the didactic potential of the University of Rzeszów at the European level*").

2. Participation in the Program ***„NANO – Nowoczesna Atrakcyjna oferta edukacyjna Nowo Otwartego kierunku „Inżynieria Materiałowa” na Wydziale Matematyczno-Przyrodniczym Uniwersytetu Rzeszowskiego”*** ("*NANO - Modern Attractive Educational Offer of the Newly Opened major field of study "Materials Engineering" at the Faculty of Mathematics and Natural Sciences, University of Rzeszow*"). The project was co-financed by the European Social Fund under the Human Capital Operational Programme, National Cohesion Strategy. duration: 2010-2016.

   Character of participation in the project: an author and a person leading a compensatory course in chemistry for students of Material Engineering.

## III.4. SCIENTIFIC AND RESEARCH SKILLS AND QUALIFICATIONS

| | |
|---|---|
| Specialties: | Physical chemistry: molecular spectroscopy, photochemistry, quantum chemistry |
| Techniques of experimental research | Long-term experience in laser spectroscopy techniques in supersonic molecular beams:<br>– supersonic jet especially supersonic pulsed free jet technique<br>– laser-induced fluorescence excitation spectra LIF<br>– cavity ring-down spectroscopy CRDS<br>– resonance multi-photon ionization spectroscopy with detection using time-of-flight mass spectrometry REMPI-TOF<br>Many years of experience in working with laser equipment:<br>– tunable high-resolution laser systems based on dye lasers<br>– Tunable high-resolution laser systems based on non-linear optics: mixing of optical frequencies (optical parametric oscillators OPO) and harmonic generators (SHG, THG)<br>Working with high-vacuum apparatus and techniques:<br>– high-vacuum chambers and vacuum gauges<br>– high-vacuum pump systems, based on diffusion pumps, turbomolecular pumps, Root pumps |
| Computational methods of quantum chemistry: | The ab initio quantum chemistry computations for molecules in excited electronic states using:<br>– *Complete Active Space Self-Consistent Field* CASSCF method<br>– multiconfigurational perturbation methods: 2-nd order Complete Active Space Perturbation Theory CASPT2, 3-rd order Complete Active Space Perturbation Theory CASPT3<br>– Multi-Reference Configuration Interaction MR CI and Multi-Reference Coupled Cluster MR CCSD<br>– Time-Dependent Density Functional Theory TD-DFT<br>– 2-nd order approximate perturbative Coupled Cluster method CC2<br>Experience with the quantum-chemistry software:<br>Gaussian, Molcas, Molpro, Turbomole |
| Foreign languages: | English – very good (FCE 1998), Russian - good, German – basic |

Applicant's signature